Eur. Phys. J. B **9**, 619–634 (1999)

THE EUROPEAN PHYSICAL JOURNAL B
EDP Sciences

Quantum charge density fluctuations and the $\gamma-\alpha$ phase transition in Ce*

A.V. Nikolaev[1,2,a] and K.H. Michel[1]

[1] Department of Physics, University of Antwerp, UIA, 2610 Antwerpen, Belgium
[2] Institute of Physical Chemistry of RAS, Leninskii prospect 31, Moscow, 117915, Russia

Received 19 October 1998

Abstract. We have calculated the quantum quadrupolar interaction due to charge density fluctuations of localized $4f$-electrons in $\gamma-$Ce by taking into account the angular dependence, the degeneracy of the localized $4f-$orbitals and the spin-orbit coupling. The calculated crystal field of $4f$ electronic states is in good agreement with neutron diffraction measurements. We show that orientational ordering of quantum quadrupoles drives a $\mathrm{Fm\bar{3}m} \rightarrow \mathrm{Pa\bar{3}}$ phase transition at ~ 86 K which we assign with the $\gamma-\alpha$ transformation. In the $\mathrm{Pa\bar{3}}$ phase the centers of mass of the Ce atoms still form a face centered cubic lattice. The theory accounts for the first order character of the transition and for the cubic lattice contraction which accompanies the transition. The transition temperature increases linearly with pressure. Our approach does not involve Kondo spin fluctuations as the significant process for the phase transition.

PACS. 71.10.-w Theories and models of many electron systems – 71.27.+a Strongly correlated electron systems; heavy fermions – 71.45.-d Collective effects – 64.70.Kb Solid-solid transitions

1 Introduction

While the Landau-Fermi liquid theory provides a successful description of conventional metals, it has become increasingly clear that the behavior of many complex materials, such as cuprate superconductors and certain transition metals, lies outside the well-explored properties, suggesting that fundamentally novel and unexpected phenomena of metallic behavior occur. Since all these materials besides conventional itinerant metallic states are characterized by localized (and degenerate) electronic states ($3d$ or $4f$), it is important to understand the peculiarities connected with them.

In this paper we want to study the direct Coulomb interaction which arises due to charge density fluctuations between degenerate localized states. We apply and extend the formalism [1–3], which initially was developed for the description of orientation dependent properties in molecular crystals, to the description of degenerate $4f$-orbitals of pristine metallic cerium.

Metallic cerium has been much studied because of its unique pressure-induced isostructural (fcc to fcc) $\gamma-\alpha$ first-order phase transition [4]. The transition accompanied by an $\approx 15\%$ volume collapse, occurs at a pressure of 8 kbar at room temperature, and the $\gamma-\alpha$ phase boundary ends in a critical point (~ 550 K, ~ 18 kbar). The physical properties of the two phases are different. For example, in the γ phase the magnetic susceptibility $\chi(T)$ follows a Curie-Weiss law, indicative of a $4f$-derived local magnetic moment close to that of the ${}^2\mathrm{F}_{5/2}$ ground state of a Ce^{3+} ion. In the collapsed α phase the overall temperature dependence of χ is very weak compared with that of the γ phase suggesting that α-Ce is basically a Pauli paramagnet and the local moments disappear [5,6,4]. However, the susceptibility χ is 'enhanced' by a factor 2-4 in comparison with the value χ_0 deduced from electronic specific heat data [5–7].

In a first interpretation [8] ('promotional' model) the localized $4f$ electrons are believed to be transferred to the $(6s5d)^3$ conduction band in α-Ce. In contrast to this model, positron annihilation experiments which probe the electron density have shown that there is no substantial difference in the number of $4f$ electrons in the two phases [9].

On the basis of thermodynamic consideration of cohesive properties Johansson proposed to describe the $\gamma-\alpha$ phase transition as a Mott transition for the $4f$-electron subsystem without significant modification of the $4f$ occupation number [10]. Though in agreement with some experimental observations [9,11], the concept of a Mott-like transition for the cerium electronic $4f$-subsystem has severe internal difficulties since delocalization of f-orbitals in the α phase would involve huge energy transformations in cerium, of the order of the Coulomb on-site repulsion parameter U_{ff} which by several orders of magnitude exceeds the characteristic energy of 100–200 K.

---

* Dedicated to Heinz Horner on the occasion of his 60th birthday.

[a] e-mail: `alex@uia.ua.ac.be`

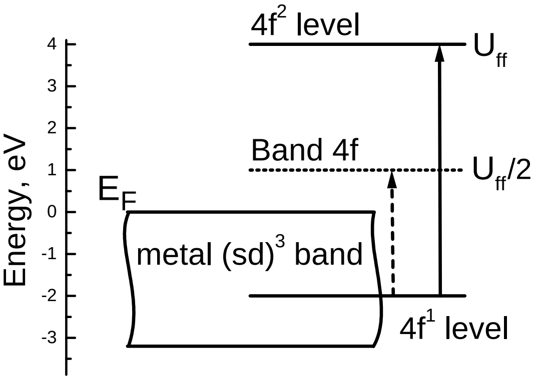

Fig. 1. Schematic energy diagram of the ground state of metallic cerium. Solid arrow indicates energy difference between $4f^1$ and $4f^2$ configurations, $U_{ff} \approx 6$ eV. Dashed arrow indicates energy loss of Coulomb energy for hypothetical delocalization of f-states, $U_{ff}/2 \approx 3$ eV.

Subsequent photoemission [12–14] and bremsstrahlung isochromat spectroscopy (BIS) [15,16], as well as X-ray absorption [17], Compton scattering measurements [11] and positron annihilation [9] confirmed a $4f^1 \to 4f^0 + \mathrm{e}^-$ peak far away (≈ 2 eV) from E_F and suggested a $4f$ occupation nearly equal to one on both sides of the transition. These results are summarized in Figure 1, where schematically the ground state of metallic cerium is shown.

The most accepted interpretation of the electronic properties of cerium, and of its metallic compounds, has been worked out on the basis of the Anderson model [18]. According to the degenerate Anderson model, the hybridization of the strongly correlated atomic-like f orbitals with the conduction band leads to a singlet nonmagnetic ground state which is separated by the Kondo energy $k_\mathrm{B} T_\mathrm{K}$ from a manifold of excited magnetic $4f$ states [19,20]. Gunnarsson and Schönhammer proposed a model [19] based on the Anderson approach, which has been widely used for a semiquantitative interpretation of Ce-based compounds [21]. In contrast to the Mott-like interpretation of the phase transition [10], a localized nature of f-states in both γ and α phases of cerium is assumed. The transition itself is explained in terms of the properties of a 'Kondo' Ce impurity. According to the Kondo volume collapse (KVC) scenario [22–24], the transition and the volume collapse are driven by the free-energy gain associated with spin fluctuations. Although the KVC theory explains the disappearance of the local moments, it is unable to specify the order parameter. Therefore, the existence of phases with other crystal symmetry (the tetragonal [25,4] and the orthorhombic [26,4] α' phase) is unaccounted for. In addition the physical mechanism driving the phase transition remains unclear. In fact, it is the postulated volume dependence of the Kondo characteristic parameter J/D [22,24] or of the averaged hybridization parameter $\pi|V(\epsilon)|^2$ [27,23], which leads to a van der Waals-like equation of state and gives isotherms similar to the liquid-gas transition.

The 'Kondo scenario' had become widely used for the interpretation of a large amount of spectroscopic data during the last decade [28,16,21]. However, recent photoemission results revealed unexpected discrepancies [29–33]. It then was concluded that the treatment of references [19,20] is irrelevant for the interpretation of strongly correlated electron systems. The temperature invariance of photoemission spectra of Ce heavy fermions [29] and of Yb-based compounds [31] as well as narrow band behavior near the Fermi energy [32] gave new impulse to the Mott-like interpretation of the $\gamma-\alpha$ phase transition in cerium [34,35]. However, this viewpoint is not widely accepted and both experimental data and their interpretation are the object of intense discussion [21,34,36].

In this paper we present an alternative to the Kondo and the Mott transitions picture of the $\gamma-\alpha$ phase transformation. Our approach is based on the existence of repulsive orientational interactions between quadrupolar charge density fluctuations. These fluctuations are formed because of quantum transitions between degenerate localized f-states of cerium. Quadrupolar (Q) charge density fluctuations are orientationally anisotropic and are classified according to $\mathrm{E_g}$ and $\mathrm{T_{2g}}$ irreducible representations of the cubic point group $\mathrm{O_h}$. We find that quadrupolar ordering leads to an antiferrorotational configuration of space group $\mathrm{Pa\bar{3}}$ while the centers of mass positions of the Ce atoms still occupy face centered cubic (fcc) lattice sites in the α phase.

Quadrupolar orderings have been observed in a number of cerium compounds such as CeAg [37], $\mathrm{CeB_6}$ [38], and its diluted alloy $\mathrm{Ce}_x\mathrm{La}_{1-x}\mathrm{B}_6$ [39]. Quadrupolar couplings are also discussed in connection with metamagnetism in other lanthanide-based intermetallic systems [40]. In case of CeAg the quadrupolar ordering was analyzed [37] on the basis of a mean field Hamiltonian, which includes the direct quadrupolar-quadrupolar interaction and a coupling of quadrupoles with lattice distortions. In the disordered phase the free energy was obtained using a susceptibility formalism. In case of $\mathrm{CeB_6}$ a few mechanisms have been proposed utilizing the interplay between spin and orbital ordering [41] or between magnetic and quadrupolar ordering [38,42] at low temperatures. In this paper we present the microscopic approach which allows us to obtain the crystal field effects, the quadrupolar coupling, Landau free energy and lattice distortions on equal footing. It should be emphasized that in the present theory we consider charge density ordering which distinguishes our approach from the model of reference [41] and others where concepts of orbital ordering [43] are employed.

2 The ground state of $\gamma-$Ce and main interactions

We start with description of the high temperature phase, that is $\gamma-$Ce. The ground state configuration of a neutral cerium atom is $[\mathrm{Xe}]4f^1 5d^1 6s^2$. The maximum of the $4f$-radial distribution function $4\pi r^2 |R_{l=3}(r)|^2$ (where $R_{l=3}(r)$ is the radial part of the $4f$ wave function and r

is radius) is at $r_{\rm max} = 0.71$ a.u. (atomic units), which is substantially smaller than the metallic radius of cerium ($R_{\rm m} \approx 3.45$ a.u.) and the corresponding radii of the other valence electrons (3.69 a.u. for $6s$ and 2.16 a.u. for $5d$). On the other hand, calculations of the on-site repulsive Coulomb integrals yield that $U_{ss}/2 = 2.87$ eV for $6s$ wave function $U_{dd}/2 = 4.27$ eV for $5d$ wave function while for $4f$-state it reaches the value $U_{ff}/2 = 11.64$ eV [44]. Not surprisingly, the valence electrons form two electronic subsystems in metallic cerium. Valence electrons of $6s$ and $5d$ type easily mix and give a Landau type Fermi liquid while $4f$ electrons preserve atomic-like behavior. In the γ and α phase two $6s$ electrons and one $5d$ electron form a conventional electronic conduction band $(6s5d)^3$ while the fourth valence electron is described by atomic-like $4f$ orbitals. Therefore, we assume that the $4f-$electrons remain localized throughout the $\gamma-\alpha$ phase transition and rule out a Mott-transition like interpretation.

In such composite electronic system we distinguish two main groups of interactions, the on-site (OS) and the intersite (IS) ones. The group of OS interactions also consists of two parts. First, there is the electronic interaction between itinerant band $(6s5d)^3$ electrons. (If it is not specified explicitly by the general term of 'electronic interaction' we mean Coulomb and exchange interactions in accordance with the Hartree-Fock approach.) In addition, there is the interaction between the band electrons and localized $4f$ electrons. On this stage we have to take into account strong electron Coulomb and exchange interactions. It is possible to go further and include correlation effects by considering several Slater determinants (multiconfigurational Hartree-Fock approach). In the following we assume the on-site correlation effects which occur in both γ and α phases are similar and most of the small energy associated with correlations cancels out in the difference. Therefore, we exclude from consideration configurations with two f^2 and zero f^0 occupation of $4f$-shell as insignificant. (Such correlations are considered as important in the Gunnarsson and Schönhammer model [19].) As we shall see our approach does not depend on particular details of the ground state. The crucial assumption (confirmed by experiment) is that in γ-Ce there exists a conventional metallic $(6s5d)^3$ band and a single $4f$ electron, which is associated with the orbital angular dependence of Y_3^m $(m = -3, ..., 3)$ spherical harmonics.

Secondly, we have inter-site interactions within the subsystem of localized $4f$ orbitals. Expanding the Coulomb inter-site interaction in multipole series we find that the first nonvanishing contribution is due to the quadrupolar interaction, Q–Q. In principle in this group, we can also include direct inter-site exchange interactions. Such interactions have been considered by Ohkawa [41] for CeB$_6$. However, since the quadrupolar inter-site coupling is larger than its inter-site exchange partner (normally the direct Coulomb interaction is stronger than the corresponding exchange), as a first approximation we omit the exchange interactions and the corresponding magnetic effects. This is in accordance with experimental observations that in β-Ce the antiferromagnetic ordering occurs at 12.45 and 13.7 K for two distinct cerium sites [4]. These temperatures are substantially lower than the transition temperature of the $\gamma-\alpha$ transformation, $\sim 100-170$ K.

The description of the anisotropic Q–Q interaction and of its consequences, which so far have not been considered in the Hartree-Fock scheme and in density functional (DFT) approaches, is the main goal of the present paper. In this Section and Appendix A we will show that a part of multipolar interactions can be reduced to a single particle term giving rise to the crystal field effects. In Section 3 we will see that the quadrupolar Q–Q interaction becomes maximum and attractive at the X point of the Brillouin zone, which leads to a quadrupolar order with space group Pa$\bar{3}$. Interactions of the quadrupoles with the conduction electrons (Q–I interactions) could lead in principle to a screening of the Q–Q interaction. We will show by symmetry arguments (Appendix B) that the Q–I interaction is inefficient at the X point of the Brillouin zone.

We consider a face centered cubic crystal of N Ce atoms with nuclear positions $\mathbf{X}(\mathbf{n})$, $\mathbf{n} = 1 - N$. We assume that the corresponding $4f$ electrons have coordinates $\mathbf{R}(\mathbf{n}) = \mathbf{X}(\mathbf{n}) + \mathbf{r}(\mathbf{n})$ and are localized on spheres with radius $|\mathbf{r}(\mathbf{n})| = r_f = 1.378$ a.u. Therefore, as a first approximation we reduce the $4f$-radial dependence to that described by the characteristic radius r_f. Notice, that if the radial dependence is taken into account then an appreciable contribution to the Coulomb repulsion between two neighboring $4f$ electrons is due to 'tail' $(r > r_{\rm max})$ or close contact regions of their wave functions. In order to reproduce correctly the intersite repulsion these regions with $r > r_{\rm max}$ have to be taken with a larger weight and we have chosen $r_f \sim \sqrt{\langle r^2 \rangle_{4f}} = \sqrt{\int r^2 R^{(\gamma)}_{l=3}(r)\, 4\pi r^2\, dr}$, where $R^{(\gamma)}_{l=3}(r)$ is the radial part of the $4f$-wave function in the γ phase [45]. Then, in describing the $4f$ electrons, we will take into account only the angular and spin parts of the atomic orbitals.

We consider the spherical harmonics $Y_l^m(\hat{\mathbf{n}}) = \langle \hat{\mathbf{n}} | l, m \rangle$ with the phase convention of reference [46], where $\hat{\mathbf{n}}$ is the unit vector in direction $\mathbf{r}(\mathbf{n})$ with polar angles $\Omega(\mathbf{n}) = (\Theta(\mathbf{n}), \varphi(\mathbf{n}))$. It is convenient to use real spherical harmonics $Y_l^{m,c}(\hat{\mathbf{n}})$, $Y_l^{m,s}(\hat{\mathbf{n}})$, $Y_l^0(\hat{\mathbf{n}})$:

$$\langle \hat{\mathbf{n}} | l, (m,c) \rangle = \frac{1}{\sqrt{2}} (\langle \hat{\mathbf{n}} | l, m \rangle + \langle \hat{\mathbf{n}} | l, -m \rangle), \quad (2.1a)$$

$$\langle \hat{\mathbf{n}} | l, (m,s) \rangle = \frac{-i}{\sqrt{2}} (\langle \hat{\mathbf{n}} | l, m \rangle - \langle \hat{\mathbf{n}} | l, -m \rangle), \quad (2.1b)$$

$$\langle \hat{\mathbf{n}} | l, 0 \rangle = \langle \hat{\mathbf{n}} | l, m = 0 \rangle. \quad (2.1c)$$

The electronic spin function $u(s_z)$ is $u_+ = \left[\begin{smallmatrix}1\\0\end{smallmatrix}\right]$ if the spin coordinate s_z is $+1/2$ and is $u_- = \left[\begin{smallmatrix}0\\1\end{smallmatrix}\right]$ if s_z is $-1/2$. With $l = 3$, there are seven values $m = -3, \ldots, m = +3$ and two $s_z = -1/2, +1/2$. In absence of a spin-orbit coupling and of a crystal field, the 14 states $|3, m\rangle \otimes |s_z\rangle$ are degenerate in energy, $\varepsilon(m, s_z) = \varepsilon_0$, and for convenience we set $\varepsilon_0 = 0$. For ions of lanthanides in solids the spin-orbit coupling is known to dominate crystal field effects. A discussion of spin-orbit coupling $V_{\rm so}$ is given in Appendix A. Starting with noninteracting $4f$ states of Ce in the fcc crystal we find that the main perturbation due to

Table 1. Energy spectrum of the operator $V_0(\mathbf{n})$ in the γ phase. Numbers in parentheses stand for degeneracy, Γ refers to the double valued representations of $\mathrm{O_h}$, μ labels the representations that occur more than once; $\Delta\varepsilon = 3008.1$ K.

i	Γ, μ		ε_i, in K	$(\varepsilon_i - \varepsilon_1)$, in K
1,2	Γ_7, 1	(2)	−1766.9	0.0
3-6	Γ_8, 1	(4)	−1703.0	63.9
7,8	Γ_6	(2)	1241.2	$\Delta\varepsilon$
9-12	Γ_8, 2	(4)	1299.0	$\Delta\varepsilon$+57.8
13,14	Γ_7, 2	(2)	1333.6	$\Delta\varepsilon$+92.4

the spin-orbit coupling V_{so} gives 6 fold levels with $J = 5/2$ and 8 fold levels with $J = 7/2$. The corresponding eigenfunctions $\langle \hat{\mathbf{n}} |\, l = 3,\ s = \frac{1}{2};\ J, J_z \rangle$ are given by the vector model [47] for addition of orbital ($l = 3$) and spin ($s = \frac{1}{2}$) momenta and transform according to double valued representations $D_{\frac{5}{2}}$ and $D_{\frac{7}{2}}$.

In a cubic crystal, these degeneracies are further lifted and one obtains three doublets (two of symmetry Γ_7 and one of Γ_6) and two quartets of symmetry Γ_8, in correspondence with the scheme [48]

$$D_{\frac{5}{2}} \to \Gamma_7 + \Gamma_8, \tag{2.2a}$$

$$D_{\frac{7}{2}} \to \Gamma_6 + \Gamma_7 + \Gamma_8. \tag{2.2b}$$

We recall that Γ_6, Γ_7 and Γ_8 are irreducible representations of the double cubic group O'_{h}. The associated 14 eigenvalues ε_i and eigenfunctions $\langle \hat{\mathbf{n}} | i \rangle$ are given by diagonalization (see Appendix A) of the corresponding matrix of the single particle potential operator

$$V_0 = V_{\mathrm{so}} + V_{\mathrm{CF}}. \tag{2.3}$$

Here V_{CF} stands for the crystal electric field potential which has the unit symmetry of the point group $\mathrm{O_h}$. It is the potential experienced by a single $4f$ electron when spherically symmetric Coulomb contributions from nuclei $V_{\mathrm{CF}}^{(\mathrm{n})}$, core electronic shells $V_{\mathrm{CF}}^{(\mathrm{core})}$, conduction electrons $V_{\mathrm{CF}}^{(\mathrm{c})}$ and $4f$ electrons $V^{(f)}$ at the twelve neighboring sites are taken into account:

$$V_{\mathrm{CF}} = V_{\mathrm{CF}}^{(\mathrm{n})} + V_{\mathrm{CF}}^{(\mathrm{core})} + V_{\mathrm{CF}}^{(\mathrm{c})} + V_{\mathrm{CF}}^{(f)}. \tag{2.4}$$

Below in this section we will calculate $V_{\mathrm{CF}}^{(f)}$ and in Appendix A we specify the other contributions. We quote the calculated energy levels ε_i in Table 1 and discuss V_{so}, V_{CF} and V_0 in Appendix A. In the following we will label the calculated eigenfunctions $\langle \hat{\mathbf{n}} | i \rangle$ and the eigenvalues ε_i by the index $i = 1 - 14$ as it is shown in Table 1. Our calculations of the crystal field effects are in good agreement with neutron diffraction measurements [49] which show that the Γ_8 quartet is 67 K above the ground state Γ_7 doublet. Recent neutron diffraction experiments [7] gave a similar value of 5.5 ± 0.5 meV (63.8 ± 5.8 K).

Interactions between $4f$ electrons at different sites will cause transitions between the quantum states i. We denote the state kets at site $\mathbf{n}$ by $|i\rangle_{\mathbf{n}}$. We will use

$$\sum_{i=1}^{14} |i\rangle_{\mathbf{n}} \langle i|_{\mathbf{n}} = 1, \qquad {}_{\mathbf{n}}\langle i | j \rangle_{\mathbf{n}'} = \delta_{ij}\, \delta_{\mathbf{n}\,\mathbf{n}'}. \tag{2.5}$$

Since

$$V_0(\mathbf{n})\, |i\rangle_{\mathbf{n}} = \varepsilon_i\, |i\rangle_{\mathbf{n}}, \tag{2.6}$$

we obtain

$$V_0(\mathbf{n}) = \sum_i |i\rangle_{\mathbf{n}}\, \varepsilon_i\, \langle i|_{\mathbf{n}}. \tag{2.7}$$

We consider the intersite ($\mathbf{n} \neq \mathbf{n}'$) Coulomb interaction between $4f$ electrons:

$$U^{(f)} = \frac{1}{2} \sum_{\mathbf{n},\mathbf{n}'} V(\mathbf{n}, \mathbf{n}'), \tag{2.8a}$$

$$V(\mathbf{n}, \mathbf{n}') = \frac{1}{|\mathbf{R}(\mathbf{n}) - \mathbf{R}(\mathbf{n}')|}, \tag{2.8b}$$

with charge units $e = 1$. We expand in terms of symmetry adapted functions [46] (SAF's) which transform as irreducible representations of the cubic site group $\mathrm{O_h}$:

$$V(\mathbf{n}, \mathbf{n}') = \sum_{l\,l'} \sum_{\tau\,\tau'} v_{l\,l'}^{\tau\,\tau'}(\mathbf{n} - \mathbf{n}')\, S_l^{\tau}(\hat{\mathbf{n}})\, S_{l'}^{\tau'}(\hat{\mathbf{n}}'). \tag{2.9}$$

The SAF's $S_l^{\tau}(\hat{\mathbf{n}})$ are symmetry adapted linear combinations of spherical harmonics [46]. The index τ stands for (Γ, μ, k), where Γ denotes the irreducible representation, μ labels the representations that occur more than once and k denotes the rows of a given representation. The argument $\mathbf{n}$ stands again for $\Omega(\mathbf{n})$ of the radius vector $\mathbf{r}(\mathbf{n})$. The coefficients $v_{l\,l'}^{\tau\,\tau'}$ are defined by

$$v_{l\,l'}^{\tau\,\tau'}(\mathbf{n}-\mathbf{n}') = \int \mathrm{d}\Omega(\mathbf{n})\mathrm{d}\Omega(\mathbf{n}') \frac{1}{|\mathbf{R}(\mathbf{n})-\mathbf{R}(\mathbf{n}')|} S_l^{\tau}(\hat{\mathbf{n}}) S_{l'}^{\tau'}(\hat{\mathbf{n}}') \tag{2.10}$$

where $\mathrm{d}\Omega = \sin\Theta\, \mathrm{d}\Theta\, \mathrm{d}\varphi$. We rewrite (2.9) in the state space of $4f$ electrons:

$$V(\mathbf{n}, \mathbf{n}') = \sum |i\rangle_{\mathbf{n}} \langle j|_{\mathbf{n}}\, v_{ij,\, i'j'}(\mathbf{n}-\mathbf{n}') |i'\rangle_{\mathbf{n}'} \langle j'|_{\mathbf{n}'}\,, \tag{2.11}$$

with summation over the initial states i, i' and final states j, j'. Here

$$v_{ij,\, i'j'}(\mathbf{n} - \mathbf{n}') = \sum c_l^{\tau}(ij)\, c_{l'}^{\tau'}(i'j')\, v_{l\,l'}^{\tau\,\tau'}(\mathbf{n} - \mathbf{n}'), \tag{2.12}$$

with summation over l, l', τ, τ' and where

$$c_l^{\tau}(ij) = \langle i | S_l^{\tau} | j \rangle = \int \mathrm{d}\Omega\, \langle i | \hat{\mathbf{n}} \rangle S_l^{\tau}(\hat{\mathbf{n}}) \langle \hat{\mathbf{n}} | j \rangle \tag{2.13}$$

are electronic multipole transition matrix elements. Notice that $c_l^{\tau}(ij)$ is independent of the site. If S_l^{τ} is chosen to

Table 2. Calculated coefficients $\langle l,(m)|S^{\tau}_{l=2}|l',(m')\rangle$, $\tau = (\mathrm{E_g},k)$, $(\mathrm{T_{2g}},k)$, $l = l' = 3$, $(m),(m')$ stand for (m,c) or (m,s) of real spherical harmonics, (2.1a-2.1c); $\langle b|S^{\tau}_{l=2}|b'\rangle = \langle l,(m)|S^{\tau}_{l=2}|l',(m')\rangle\delta_{s_z\,s'_z}$, and s_z, s'_z are spin components. Those functions which are not shown in this Table give zero contributions to all $S^{\tau}_{l=2}$ functions.

(m)	(m')	$(\mathrm{T_{2g}},1)$	$(\mathrm{T_{2g}},2)$	$(\mathrm{T_{2g}},3)$	$(\mathrm{E_g},1)$	$(\mathrm{E_g},2)$
0	0	0	0	0	0.16821	0
0	(1,c)	0	0.05947	0	0	0
0	(2,c)	0	0	0	0	−0.18806
0	(1,s)	0.05947	0	0	0	0
0	(2,s)	0	0	−0.18806	0	0
(1,c)	(1,c)	0	0	0	0.12616	0.14567
(1,c)	(2,c)	0	0.11516	0	0	0
(1,c)	(3,c)	0	0	0	0	−0.09403
(1,c)	(1,s)	0	0	0.14567	0	0
(1,c)	(2,s)	0.11516	0	0	0	0
(1,c)	(3,s)	0	0	−0.09403	0	0
(2,c)	(3,c)	0	0.14868	0	0	0
(2,c)	(1,s)	−0.11516	0	0	0	0
(2,c)	(3,s)	0.14868	0	0	0	0
(3,c)	(3,c)	0	0	0	−0.21026	0
(3,c)	(1,s)	0	0	0.09403	0	0
(3,c)	(2,s)	−0.14868	0	0	0	0
(1,s)	(1,s)	0	0	0	0.12616	−0.14567
(1,s)	(2,s)	0	0.11516	0	0	0
(1,s)	(3,s)	0	0	0	0	−0.09403
(2,s)	(3,s)	0	0.14868	0	0	0
(3,s)	(3,s)	0	0	0	−0.21026	0

be real [46] then $c^{\tau}_{l}(ij)^{*} = c^{\tau}_{l}(ji)$. Since $|i\rangle$ and $|j\rangle$ refer to orbitals with $l = 3$, we see that only functions $c^{\tau}_{l}(ij)$ with l even can differ from zero. If we consider another orthonormalized basis with state vectors $|b\rangle$, $b = 1-14$ then

$$\begin{aligned} c^{\tau}_{l}(ij) &= \sum_{b\,b'}\langle i|b\rangle\langle b|S^{\tau}_{l}|b'\rangle\langle b'|j\rangle \\ &= \sum_{b\,b'}\langle i|b\rangle c^{\tau}_{l}(b\,b')\langle b'|j\rangle, \end{aligned} \tag{2.14}$$

where $\langle i|b\rangle$ determines a unitary matrix of transformation and where the coefficients $c^{\tau}_{l}(b\,b')$ are given in this new basis. In Table 2 we quote the electronic quadrupolar matrix elements $c^{\tau}_{l=2}(b\,b')$ for the basis with real spherical harmonics (A.15) which is defined in Appendix A. Since the multipolar integral (2.10) varies like $|\mathbf{R}(\mathbf{n}) - \mathbf{R}(\mathbf{n}')|^{-(l+l'+1)}$, we will restrict ourselves to nearest neighbor interactions on the fcc lattice, in addition we will retain only the lowest values of l and l'. Notice that by symmetry dipolar ($l = 1$) matrix elements between $4f$ states are zero.

Table 3. Calculated parameters $v^{\tau\tau'}_{22}(\mathbf{n}-\mathbf{n}')$, $\tau,\tau' = \mathrm{T_{2g}}$, in K. First site coordinates ($\mathbf{n}$) are $(0,0,0)$. Last column refers to labels of corresponding matrix elements used in reference [50].

S^{τ}_{2}	$\mathbf{n}'$	$S^{\tau'}_{2}$	$\gamma{-}$Ce	$\alpha{-}$Ce	Ref. [50]
$Y^{1,s}_{2}$	$(0,\frac{1}{2},\frac{1}{2})$	$Y^{1,s}_{2}$	872.6	1190.7	γ
$Y^{1,s}_{2}$	$(\frac{1}{2},\frac{1}{2},0)$	$Y^{1,s}_{2}$	−275.6	−376.0	α
$Y^{1,s}_{2}$	$(\frac{1}{2},\frac{1}{2},0)$	$Y^{1,c}_{2}$	−459.3	−626.7	$-\beta$

Table 4. Calculated parameters $v^{\tau\tau'}_{22}(\mathbf{n}-\mathbf{n}')$, $\tau,\tau' = \mathrm{E_g}$, in K. First site coordinates ($\mathbf{n}$) are $(0,0,0)$.

S^{τ}_{2}	$\mathbf{n}'$	$S^{\tau'}_{2}$	$\gamma{-}$Ce	$\alpha{-}$Ce	Ref. [50]
Y^{0}_{2}	$(0,\frac{1}{2},\frac{1}{2})$	Y^{0}_{2}	−447.8	−611.0	r
Y^{0}_{2}	$(\frac{1}{2},\frac{1}{2},0)$	Y^{0}_{2}	413.4	564.0	p
Y^{0}_{2}	$(0,\frac{1}{2},\frac{1}{2})$	$Y^{2,c}_{2}$	−497.2	−678.4	t
$Y^{2,c}_{2}$	$(0,\frac{1}{2},\frac{1}{2})$	$Y^{2,c}_{2}$	126.3	172.3	s
$Y^{2,c}_{2}$	$(\frac{1}{2},\frac{1}{2},0)$	$Y^{2,c}_{2}$	−734.8	−1002.7	q

Table 5. Calculated parameters $v^{\tau\tau'}_{22}(\mathbf{n}-\mathbf{n}')$, $\tau = \mathrm{T_{2g}}$ for $\mathbf{n}$, $\tau' = \mathrm{E_g}$ for $\mathbf{n}'$, in K. First site coordinates ($\mathbf{n}$) are $(0,0,0)$.

S^{τ}_{2}	$\mathbf{n}'$	$S^{\tau'}_{2}$	$\gamma{-}$Ce	$\alpha{-}$Ce	Ref. [50]
$Y^{1,s}_{2}$	$(0,\frac{1}{2},\frac{1}{2})$	Y^{0}_{2}	98.9	271.3	$-\lambda$
$Y^{1,s}_{2}$	$(0,\frac{1}{2},\frac{1}{2})$	$Y^{2,c}_{2}$	−171.3	−470.0	$-\mu$
$Y^{2,s}_{2}$	$(\frac{1}{2},\frac{1}{2},0)$	Y^{0}_{2}	−197.8	−542.7	$-\nu$

Similar to the situation for multipolar interactions in molecular crystals [2,3], we distinguish interactions where both l and l' are different from zero from those where $l \neq 0$, but $l' = 0$. The first ones are the orientational pair interactions and from symmetry it follows that the lowest allowed values are $l = 2$ and $l' = 2$, *i.e.* quadrupoles. The quadrupolar SAF's consist of a doublet of $\mathrm{E_g}$ symmetry, $S^{\mathrm{E_g},k}_{2}(\hat{\mathbf{n}})$, $k = 1,2$:

$$\langle\hat{\mathbf{n}}|\mathrm{E_g},1\rangle = \langle\hat{\mathbf{n}}|2,0\rangle, \tag{2.15a}$$

$$\langle\hat{\mathbf{n}}|\mathrm{E_g},2\rangle = \langle\hat{\mathbf{n}}|2,(2,c)\rangle, \tag{2.15b}$$

and a triplet of $\mathrm{T_{2g}}$ symmetry, $S^{\mathrm{T_{2g}},k}_{2}(\hat{\mathbf{n}})$, $k = 1-3$:

$$\langle\hat{\mathbf{n}}|\mathrm{T_{2g}},1\rangle = \langle\hat{\mathbf{n}}|2,(1,s)\rangle, \tag{2.16a}$$

$$\langle\hat{\mathbf{n}}|\mathrm{T_{2g}},2\rangle = \langle\hat{\mathbf{n}}|2,(1,c)\rangle, \tag{2.16b}$$

$$\langle\hat{\mathbf{n}}|\mathrm{T_{2g}},3\rangle = \langle\hat{\mathbf{n}}|2,(2,s)\rangle. \tag{2.16c}$$

The calculated values of the matrix elements $v^{\tau\tau'}_{22}(\mathbf{n}-\mathbf{n}')$, (2.10), are quoted in Tables 3-5. We took $a = 9.753$ a.u. for $\gamma{-}$Ce and $a = 9.165$ a.u. for α-Ce.

We will neglect electronic orientational pair interactions with higher values of l and l' and retain only the quadrupolar interaction V_{QQ}. Defining the operator

$$\rho_{ij}(\mathbf{n}) = |i\rangle_{\mathbf{n}}\langle j|_{\mathbf{n}}, \tag{2.17}$$

we obtain

$$V_{\mathrm{QQ}} = \sum \rho_{ij}(\mathbf{n})\, v^{\mathrm{QQ}}_{ij,\,i'j'}(\mathbf{n}-\mathbf{n}')\, \rho_{i'j'}(\mathbf{n}'), \tag{2.18}$$

with

$$v^{\mathrm{QQ}}_{ij,\,i'j'}(\mathbf{n}-\mathbf{n}') = \sum v_{22}^{\tau\tau'}(\mathbf{n}-\mathbf{n}')\, c_2^{\tau}(ij)\, c_2^{\tau'}(i'j'). \tag{2.19}$$

The interactions where $l \neq 0$, $l' = 0$, contribute to the crystal field V_{CF}. The crystal field has unit cubic symmetry, the lowest non trivial value of l is 4 and $\tau = (\mathrm{A_{1g}}, 1)$, where $\mathrm{A_{1g}}$ is the unit representation of $\mathrm{O_h}$. The leading coefficients are ${v_{l}^{\mathrm{A_{1g}}}}{}_{0}^{\mathrm{A_{1g}}}$, with $l = 4$, 6. Notice that

$$c_0^{\mathrm{A_{1g}}}(i'j') = \frac{1}{\sqrt{4\pi}}\delta_{i'\,j'}. \tag{2.20}$$

We then obtain

$$\begin{aligned} V_{\mathrm{CF}}^{(f)}(\mathbf{n}) &= \sum_{\mathbf{n}'} V_{\mathrm{CF}}^{(f)}(\mathbf{n},\mathbf{n}') \\ &= \frac{12}{\sqrt{4\pi}} \sum_{l} {v_{l}^{\mathrm{A_{1g}}}}{}_{0}^{\mathrm{A_{1g}}} \sum_{ij} \rho_{ij}(\mathbf{n}) c_l^{\mathrm{A_{1g}}}(ij). \end{aligned} \tag{2.21}$$

Notice that ${v_{l}^{\mathrm{A_{1g}}}}{}_{0}^{\mathrm{A_{1g}}}$ as a consequence of cubic symmetry, is the same for all 12 nearest neighbors $\mathbf{n}'$ of a given site $\mathbf{n}$, and as a consequence of lattice translational symmetry, is independent of $\mathbf{n}$. With the separation of $V(\mathbf{n},\mathbf{n}')$ in V_{QQ} and $V_{\mathrm{CF}}^{(f)}$, we obtain

$$U^{(f)} = U_{\mathrm{QQ}}^{(f)} + U_{\mathrm{CF}}^{(f)}, \tag{2.22a}$$

where

$$U_{\mathrm{QQ}}^{(f)} = \frac{1}{2}\sum_{\mathbf{n},\,\mathbf{n}'} V_{\mathrm{QQ}}(\mathbf{n},\mathbf{n}'), \tag{2.22b}$$

$$U_{\mathrm{CF}}^{(f)} = \sum_{\mathbf{n}} V_{\mathrm{CF}}^{(f)}(\mathbf{n}). \tag{2.22c}$$

Taking into account the other contribution to the crystal field V_{CF}, equation (2.4), and the spin-orbit coupling V_{so}, the total potential of the $4f$ electron system is given by

$$U = U_{\mathrm{QQ}}^{(f)} + U_0, \tag{2.23}$$

where

$$U_0 = \sum_{\mathbf{n}} V_0(\mathbf{n}), \tag{2.24}$$

with V_0 given by equation (2.3). Expressing V_0, (2.7), in terms of ρ_{ij} we find

$$V_0(\mathbf{n}) = \sum_{i} \rho_{ii}(\mathbf{n})\varepsilon_i. \tag{2.25}$$

In Appendix B we show that the anisotropic quadrupolar interaction cannot be screened by the inner closed shells or by the conduction band electrons. The electronic densities associated with closed shells or with the conduction band are essentially isotropic.

In the next section we will study the collective orientational behavior which follows from the potential U, equation (2.23).

3 Phase transition

Here we will discuss the transition $\mathrm{Fm\bar{3}m} \rightarrow \mathrm{Pa\bar{3}}$ of the $4f$ quadrupoles. In order to study collective phenomena we introduce Fourier transforms of the electronic density operator:

$$\rho_{ij}(\mathbf{q}) = \frac{1}{\sqrt{N}} \sum_{\mathbf{n}} \mathrm{e}^{i\mathbf{q}\cdot\mathbf{X}(\mathbf{n})} \rho_{ij}(\mathbf{n}), \tag{3.1}$$

where $\mathbf{q}$ is the wave vector. The orientational pair interaction now reads

$$U_{\mathrm{QQ}}^{(f)} = \frac{1}{2}\sum_{\mathbf{q}}\sum \rho_{ij}(\mathbf{q})\, v^{\mathrm{QQ}}_{ij,\,i'j'}(\mathbf{q})\, \rho^{\dagger}_{i'j'}(\mathbf{q}), \tag{3.2}$$

where

$$v^{\mathrm{QQ}}_{ij,\,i'j'}(\mathbf{q}) = \sum_{\tau\,\tau'} v_{22}^{\tau\tau'}(\mathbf{q})\, c_2^{\tau}(ij)\, c_2^{\tau'}(i'j')^{*}, \tag{3.3a}$$

with

$$v_{22}^{\tau\tau'}(\mathbf{q}) = \sum_{\mathbf{h}} \mathrm{e}^{i\mathbf{q}\cdot\mathbf{X}(\mathbf{h})} v_{22}^{\tau\tau'}(\mathbf{h}). \tag{3.3b}$$

The matrix $v_{22}^{\tau\tau'}(\mathbf{q})$ is given by explicit expressions (A1, A6) and (A7) of reference [50], while the corresponding interaction parameters (α, β, …) are cited in Tables 3-5. We diagonalize the 5×5 matrix $v_{22}(\mathbf{q})$ and write

$$v_{22}^{\tau\tau'}(\mathbf{q}) = \sum_{\alpha=1}^{5} e_{\alpha}^{*}(\tau,\mathbf{q})\, \lambda_{\alpha}(\mathbf{q})\, e_{\alpha}(\tau',\mathbf{q}), \tag{3.4}$$

where $\lambda_{\alpha}(\mathbf{q})$ are the eigenvalues and $e_{\alpha}(\mathbf{q})$ the eigenvectors. We have studied the eigenvalue spectrum throughout the Brillouin zone. We find that the largest negative eigenvalue, which is $\lambda_{\mathrm{X}_2^+} = -3950$ K, occurs at the X point of the Brillouin zone ($\mathbf{q}_x^{\mathrm{X}} = (2\pi/a)(1{,}0{,}0)$, etc., where $a = 9.753$ a.u. is the cubic lattice constant of $\gamma-$Ce) and is due to a normal mode with $\mathrm{E_g}$ components. This mode, which we call X_2^+-mode, corresponds to a basis function of the irreducible representation X_2^+ of the space group $\mathrm{Fm\bar{3}m}$, and its condensation would lead to a tetragonal structure $\mathrm{P4_2/mnm}$. The second largest negative eigenvalue ($\lambda_{\mathrm{X}_5^+} = -4\gamma = -3491$ K) is doubly degenerate and belongs to $\mathrm{T_{2g}}$ components. This mode, which we call X_5^+-mode, belongs to the irreducible representation X_5^+ of $\mathrm{Fm\bar{3}m}$ and its condensation leads to a $\mathrm{Pa\bar{3}}$ structure. Notice, that in a $\mathrm{Pa\bar{3}}$ structure the center of mass positions still form a fcc lattice and hence we consider this case to be relevant for the isostructural phase transition $\gamma \to \alpha$ in Ce. The situation is reminiscent of orientational phase transitions in molecular crystals, where a Pa$\bar{3}$ structure is associated with orientational molecular ordering while the lattice remains cubic [51,3]. In the case of Ce we propose that the quadrupolar charge density fluctuations of the $4f$ electrons orders in a Pa$\bar{3}$ structure at the transition $\gamma \to \alpha$.

Defining "orientational" normal coordinates

$$\rho^{\alpha}(\mathbf{q}) = \sum_{ij} \sum_{\tau} \rho_{ij}(\mathbf{q})\, c_2^{\tau}(ij)\, e_{\alpha}(\tau, \mathbf{q}), \qquad (3.5)$$

we rewrite expansion (3.2) as:

$$U_{\mathrm{QQ}}^{(f)} = \frac{1}{2} \sum_{\mathbf{q}} \sum_{\alpha} \rho^{\alpha}(\mathbf{q})\, \lambda_{\alpha}(\mathbf{q})\, [\rho^{\alpha}(\mathbf{q})]^{\dagger}. \qquad (3.6)$$

Which mode α condenses first at the X point depends not only on the eigenvalue but also on the value of the corresponding single particle susceptibility $y^{(2)}(\alpha)/T$ [3,50] where $y^{(2)}(\alpha) \equiv \langle \rho^{\alpha}(\mathbf{n})\, \rho^{\alpha}(\mathbf{n}) \rangle_0$. In case of a second order transition, the transition temperature would be given by

$$T_c = y^{(2)}(\alpha)\, |\lambda_{\alpha}(\mathbf{q}_x^{\mathrm{X}})|. \qquad (3.7)$$

In Appendix C we will discuss the prevalence of a transition to a Pa$\bar{3}$ structure over a transition to P4$_2$/mnm. In the following we will describe the condensation scheme for Pa$\bar{3}$ and exploit the close analogy with the orientational ordering transition [3] in solid C$_{60}$. The T$_{2\mathrm{g}}$–T$_{2\mathrm{g}}$ interaction is accounted for by a submatrix [3,50] of dimension 3 of $v_{22}(\mathbf{q})$ which becomes diagonal at $\mathbf{q}_x^{\mathrm{X}}$ with nonzero elements $[\lambda_1, \lambda_2, \lambda_3]$, where $\lambda_1 > 0$ and $\lambda_2 = \lambda_3 = -\lambda^{\mathrm{X}} \equiv \lambda_{\mathrm{X}_5^+} < 0$. Here the indices 1-3 correspond to those of equations (2.16a-2.16c). We see that the modes with row index $k = 2$ and $k = 3$ are degenerate, the corresponding eigenvectors are $\mathbf{e}(2, \mathbf{q}_x^{\mathrm{X}}) = (0,1,0)$ and $\mathbf{e}(3, \mathbf{q}_x^{\mathrm{X}}) = (0,0,1)$, respectively. We denote the corresponding normal coordinates by $\rho^{(k)}(\mathbf{q}_x^{\mathrm{X}})$, where (k) stands for $\tau = (\mathrm{T}_{2\mathrm{g}}, k)$:

$$\rho^{(k)}(\mathbf{q}_x^{\mathrm{X}}) = \sum_{ij} \rho_{ij}(\mathbf{q}_x^{\mathrm{X}})\, c_2^{(k)}(ij), \quad k = 2, 3. \qquad (3.8a)$$

Similarly at $\mathbf{q}_y^{\mathrm{X}} = (2\pi/a)(0{,}1{,}0)$ the degenerate normal coordinates with the largest eigenvector $\lambda(\mathbf{q}_y^{\mathrm{X}}) = -\lambda^{\mathrm{X}}$ are

$$\rho^{(k)}(\mathbf{q}_y^{\mathrm{X}}) = \sum_{ij} \rho_{ij}(\mathbf{q}_y^{\mathrm{X}})\, c_2^{(k)}(ij), \quad k = 1, 3, \qquad (3.8b)$$

and at $\mathbf{q}_z^{\mathrm{X}} = (2\pi/a)(0{,}0{,}1)$,

$$\rho^{(k)}(\mathbf{q}_z^{\mathrm{X}}) = \sum_{ij} \rho_{ij}(\mathbf{q}_z^{\mathrm{X}})\, c_2^{(k)}(ij), \quad k = 1, 2. \qquad (3.8c)$$

The functions $\rho^{(k)}(\mathbf{q}_{\bullet}^{\mathrm{X}})$ form a basis of the six dimensional irreducible representation X_5^+ of the space group Fm$\bar{3}$m. A possible condensation scheme for the transition Fm$\bar{3}$m $\to$ Pa$\bar{3}$ is then given by

$$\rho^{(3)\mathrm{e}}(\mathbf{q}_x^{\mathrm{X}}) = \rho^{(1)\mathrm{e}}(\mathbf{q}_y^{\mathrm{X}}) = \rho^{(2)\mathrm{e}}(\mathbf{q}_z^{\mathrm{X}}) \equiv \rho\sqrt{N} \neq 0, \qquad (3.9a)$$

$$\rho^{(2)\mathrm{e}}(\mathbf{q}_x^{\mathrm{X}}) = \rho^{(3)\mathrm{e}}(\mathbf{q}_y^{\mathrm{X}}) = \rho^{(1)\mathrm{e}}(\mathbf{q}_z^{\mathrm{X}}) = 0, \qquad (3.9b)$$

where the subscript e stands for a thermal expectation value and where ρ is the order parameter amplitude. The condensation scheme corresponds to a domain and there are eight possible domains of Pa$\bar{3}$. The quantities $\rho^{(k)}(\mathbf{q}_{\bullet}^{\mathrm{X}})$ in (3.9a) are the order parameter variables. It is convenient to write

$$\rho^{(k)\mathrm{e}}(\mathbf{q}) = \sqrt{N}\, \rho\, (\delta_{\mathbf{q},\, -\mathbf{q}_{\xi}^{\mathrm{X}}} + \delta_{\mathbf{q},\, \mathbf{q}_{\xi}^{\mathrm{X}}})/2, \qquad (3.10)$$

where $k = 1, 2, 3$ corresponds to $\xi = y, z, x$ respectively. Using the quadrupolar interaction (3.6) for T$_{2\mathrm{g}}$ modes, we obtain the mean field (MF) interaction

$$U^{\mathrm{MF}} = -\lambda^{\mathrm{X}} \rho \sqrt{N} [\rho^{(1)}(\mathbf{q}_y^{\mathrm{X}}) + \rho^{(2)}(\mathbf{q}_z^{\mathrm{X}}) + \rho^{(3)}(\mathbf{q}_x^{\mathrm{X}})]. \qquad (3.11)$$

The Pa$\bar{3}$ structure has four sublattices which contain the sites (0,0,0), $(a/2)$(0,1,1), $(a/2)$(1,0,1), $(a/2)$(1,1,0) and which we label by $\{\mathbf{n}_i\}$, $i = 1 - 4$, respectively. Taking into account equations (3.8a, 3.9a, 3.1), we have

$$\rho^{(3)}(\mathbf{q}_x^{\mathrm{X}}) = \frac{1}{\sqrt{N}} \sum_{ij} [\sum_{\mathbf{n}_1} \rho_{ij}(\mathbf{n}_1) + \sum_{\mathbf{n}_2} \rho_{ij}(\mathbf{n}_2) - \sum_{\mathbf{n}_3} \rho_{ij}(\mathbf{n}_3) - \sum_{\mathbf{n}_4} \rho_{ij}(\mathbf{n}_4)]\, c_2^{(3)}(ij), \qquad (3.12)$$

and similar expressions for $\rho^{(1)}(\mathbf{q}_y^{\mathrm{X}})$ and $\rho^{(2)}(\mathbf{q}_z^{\mathrm{X}})$. The mean field interaction on sublattice $\{\mathbf{n}_1\}$ is then given by

$$U^{\mathrm{MF}}(\mathbf{n}_1) = -\lambda^{\mathrm{X}} \rho \sum_{ij} [c_2^{(3)}(ij) + c_2^{(2)}(ij) + c_2^{(1)}(ij)]\, \rho_{ij}(\mathbf{n}_1). \qquad (3.13)$$

The order parameter components at site $\mathbf{n}$ are defined by

$$\rho^{(k)}(\mathbf{n}) = \sum_{ij} c_2^{(k)}(ij)\, \rho_{ij}(\mathbf{n}), \qquad (3.14)$$

and the mean field interaction at site $\mathbf{n}_1$ becomes

$$U^{\mathrm{MF}}(\mathbf{n}_1) = -\lambda^{\mathrm{X}} \rho\, [\rho^{(3)}(\mathbf{n}_1) + \rho^{(2)}(\mathbf{n}_1) + \rho^{(1)}(\mathbf{n}_1)]. \qquad (3.15)$$

The mean field Hamiltonian reads

$$H^{\mathrm{MF}}(\mathbf{n}_1) = U^{\mathrm{MF}}(\mathbf{n}_1) + V_0(\mathbf{n}_1), \qquad (3.16)$$

where $V_0(\mathbf{n}_1)$ is given by equation (2.25). The order parameter amplitude is obtained by solving the mean field equation

$$\rho = \frac{\mathrm{Tr}\{\rho^{(k)}(\mathbf{n}_1)\, \exp[-H^{\mathrm{MF}}(\mathbf{n}_1)/T]\}}{\mathrm{Tr}\{\exp[-H^{\mathrm{MF}}(\mathbf{n}_1)/T]\}}. \qquad (3.17)$$

Symmetry implies that this expression is independent of k. In the disordered phase, $H^{\mathrm{MF}}(\mathbf{n})$ reduces to $V_0(\mathbf{n})$. The single particle density operator then reads

$$w = \mathrm{e}^{-V_0(\mathbf{n})/T} = \sum_i \rho_{ii}\, \mathrm{e}^{-\varepsilon_i/T}, \tag{3.18}$$

and the sum of states is given by

$$\begin{aligned} Z_0 = \mathrm{Tr}(w) = 2\mathrm{e}^{-\varepsilon(\Gamma_7,1)/T} + 4\mathrm{e}^{-\varepsilon(\Gamma_8,1)/T} + 2\mathrm{e}^{-\varepsilon(\Gamma_6)/T} \\ + 4\mathrm{e}^{-\varepsilon(\Gamma_8,2)/T} + 2\mathrm{e}^{-\varepsilon(\Gamma_7,2)/T}, \end{aligned} \tag{3.19}$$

where the argument in parentheses refers to Γ, μ, Table 1. The order parameter equation (3.17) then reduces to

$$\langle \rho^{(k)} \rangle = \frac{\mathrm{Tr}\,\{w\, \rho^{(k)}(\mathbf{n})\}}{Z_0} \cdot \tag{3.20}$$

In the disordered phase one finds $\langle \rho^{(k)} \rangle = 0$, where Γ' in $(k) = (\Gamma', k)$ is one of the representations $\mathrm{T}_{2\mathrm{g}}$ or E_{g}. Indeed,

$$\mathrm{Tr}\,\{w\rho^{(k)}(\mathbf{n})\} = \sum_{\Gamma} \mathrm{e}^{-\varepsilon(\Gamma)/T} \sum_{i_\Gamma} c_2^{(k)}(i_\Gamma i_\Gamma) = 0, \tag{3.21}$$

since

$$\sum_{i_\Gamma} c_2^{(k)}(i_\Gamma i_\Gamma) = 0. \tag{3.22}$$

Here $\Gamma = \Gamma_7, 1$ ($i_\Gamma = 1, 2$); $\Gamma_8, 1$ ($i_\Gamma = 3-6$); Γ_6 ($i_\Gamma = 7, 8$); $\Gamma_8, 2$ ($i_\Gamma = 9-12$); $\Gamma_7, 2$ ($i_\Gamma = 13, 14$); see Table 1. To prove equation (3.22) we use the integral form (2.13) of $c_2^{(k)}(i_\Gamma i_\Gamma)$:

$$\begin{aligned} \sum_{i_\Gamma} c_2^{(k)}(i_\Gamma i_\Gamma) &= \int \mathrm{d}\Omega\, S^{\tau}_{l=2}(\hat{\mathbf{n}}) \sum_{i_\Gamma} \langle \hat{\mathbf{n}} | i_\Gamma \rangle^* \langle \hat{\mathbf{n}} | i_\Gamma \rangle \\ &= \int \mathrm{d}\Omega\, S^{\tau}_2(\hat{\mathbf{n}})\, {S'}^{\mathrm{A}_{1\mathrm{g}}}(\hat{\mathbf{n}}), \end{aligned} \tag{3.23}$$

where

$${S'}^{\mathrm{A}_{1\mathrm{g}}}(\hat{\mathbf{n}}) = \sum_{i_\Gamma} \langle \hat{\mathbf{n}} | i_\Gamma \rangle^* \langle \hat{\mathbf{n}} | i_\Gamma \rangle \tag{3.24}$$

is an invariant function according to generalized Unsöld theorem [48]. Therefore, the integral in (3.23) equals zero unless $\tau = \mathrm{A}_{1\mathrm{g}}$.

4 Free energy

Starting with the mean field Hamiltonian (3.16) and using methods [2,3] which are familiar from the theory of orientational phase transitions in molecular crystals, we have derived a Landau expansion [52] of the free energy F in the Pa$\bar{3}$ phase (which we associate with α-Ce). Up to fourth order we obtain

$$(F/N) = F_0/N + A\rho^2 + B\rho^3 + C\rho^4. \tag{4.1}$$

Here F_0 is the free energy (per atom) in the disordered phase:

$$F_0 = -T \ln Z_0, \tag{4.2}$$

where Z_0 is given by equation (3.19). The expansion coefficients are given by

$$A = \frac{3}{2}\left[\frac{T}{x^{(2)}} - \lambda_{\mathrm{X}}\right], \tag{4.3}$$

$$B = -T\, x^{(3)}_{123}\, [x^{(2)}]^{-3}, \tag{4.4}$$

$$C = \frac{T}{8(x^{(2)})^4}\left[9(x^{(2)})^2 - x^{(4)}_{1111} - 6x^{(4)}_{1122} + \frac{12(x^{(3)}_{123})^2}{x^{(2)}}\right]. \tag{4.5}$$

Here the quantities $x^{(j)}$, $j = 2, 3, 4$ are single particle expectation values

$$x^{(2)} = \langle (\rho^{(k)}(\mathbf{n}))^2 \rangle_0, \tag{4.6a}$$

$$x^{(3)}_{123} = \langle \rho^{(1)}(\mathbf{n})\, \rho^{(2)}(\mathbf{n})\, \rho^{(3)}(\mathbf{n}) \rangle_0, \tag{4.6b}$$

$$x^{(4)}_{1111} = \langle (\rho^{(k)}(\mathbf{n}))^4 \rangle_0, \tag{4.6c}$$

$$x^{(4)}_{1122} = \langle (\rho^{(k)}(\mathbf{n}))^2\, (\rho^{(k')}(\mathbf{n}))^2 \rangle_0, \quad k \neq k'. \tag{4.6d}$$

These quantities are calculated with the density matrix w, equation (3.18). We readily obtain

$$x^{(2)} = \left(\sum_{ij} c_2^{(k)}(ij)\, c_2^{(k)}(ji)\, \mathrm{e}^{-\varepsilon_i/T} \right) / Z_0, \tag{4.7a}$$

$$x^{(3)}_{123} = \left(\sum_{ijh} c_2^{(1)}(ij)\, c_2^{(2)}(jh)\, c_2^{(3)}(hi)\, \mathrm{e}^{-\varepsilon_i/T} \right) / Z_0, \tag{4.7b}$$

$$x^{(4)}_{1111} = \left(\sum_{ijhl} c_2^{(1)}(ij) c_2^{(1)}(jh) c_2^{(1)}(hl) c_2^{(1)}(li) \mathrm{e}^{-\varepsilon_i/T} \right) / Z_0, \tag{4.7c}$$

$$x^{(4)}_{1122} = \left(\sum_{ijhl} c_2^{(1)}(ij) c_2^{(1)}(ji) c_3^{(2)}(hl) c_4^{(2)}(li) \mathrm{e}^{-\varepsilon_i/T} \right) / Z_0. \tag{4.7d}$$

In deriving the Landau expansion for the free energy we have assumed that quantum mechanical fluctuations of the quadrupolar order parameter away from its expectation value are negligible. Such fluctuations occur in principle as a consequence of the non-commutativity of $U^{\mathrm{MF}}(\mathbf{n})$ and $V_0(\mathbf{n})$. Here we argue that they are insignificant since a large number of quadrupoles are involved in the ordering process. The expectation values (4.7a-4.7d) account for thermal fluctuations.

We now discuss the phase transition on the basis of the Landau free energy (4.1). Since the product of the three $\mathrm{T}_{2\mathrm{g}}$ components is a cubic invariant, $x^{(3)}_{123} \neq 0$, the phase

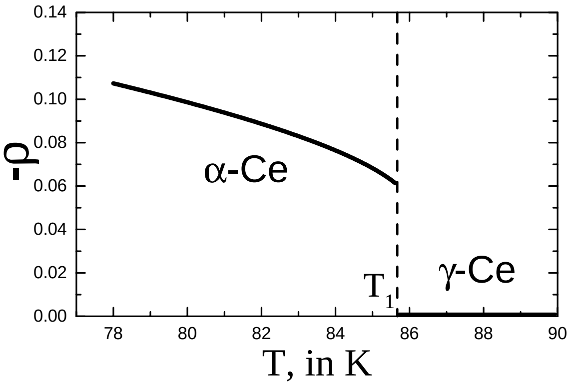

Fig. 2. Temperature dependence of the order parameter amplitude ρ.

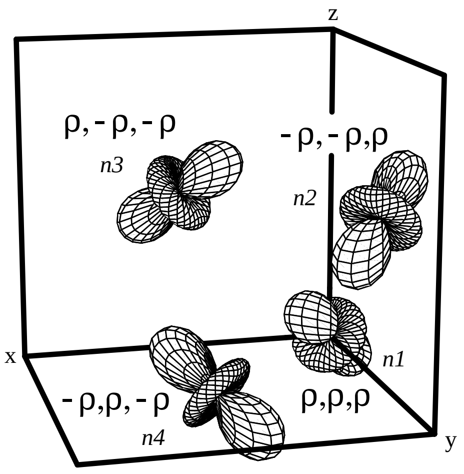

Fig. 3. The angular dependence of four functions $\{\rho^{(1)}(n)Y_2^{1,s} + \rho^{(2)}(n)Y_2^{1,c} + \rho^{(3)}(n)Y_2^{2,s}\}/\rho$ which represent quantum quadrupoles on the four sublattices $\{\mathbf{n}_s\}$ of Pa$\bar{3}$ structure, α-Ce. The order parameter components $\rho^{(k)\,\mathrm{e}}(\mathbf{n})$, equation (3.14), on the sublattices are also shown.

transition is of first order. The transition temperature is obtained from the solution of

$$T_1 = x^{(2)}(T_1)\left[\lambda^{\mathrm{X}} + \frac{B^2(T_1)}{6C(T_1)}\right]. \tag{4.8}$$

The order parameter amplitude differs from zero for $T \le T_1$

$$\rho(T) = \frac{-3B - \sqrt{9B^2 - 32AC}}{8C}, \tag{4.9}$$

with a discontinuity at T_1:

$$\rho(T_1) = -\frac{B(T_1)}{2C(T_1)}. \tag{4.10}$$

Numerical calculations (see Appendix C for details) give the transition temperature $T_1 = 85.6$ K and the order parameter discontinuity $\rho(T_1) = -0.06$, Figure 2.

Physically the phase transition consists of an ordering of the electronic quadrupolar density associated with the $4f$ electrons in a Pa$\bar{3}$ structure, see Figure 3.

Studies of thermoelastic phenomena [53] performed for the orientational phase transition in pristine C$_{60}$ which is of the same type, Fm$\bar{3}$m $\to$ Pa$\bar{3}$, show that there is a softening of the coefficient C in the Landau expansion. As a result the transition temperature T_1 will further increase and this conclusion should hold for the phase transition in cerium. However, specific estimations of this effect depend on the elastic constants at T_1 which are unknown. We recall that on cooling the $\gamma \to \alpha$ transition occurs [4] at ~ 100 K (~ 170 K on warming) and conclude that the calculated transition temperature $T_1 > 86$ K is in fair correspondence with experiment.

Early experiments [54,4] have shown that the first order phase transition line between the $\gamma-\alpha$ phases ends in a critical point at $T \sim 550$ K and $P \sim 1.8$ GPa. Within the present theory the existence of such an end point where the phase transition becomes second order would imply the vanishing of the third order coefficient B in the Landau expansion (4.1) or equivalently the vanishing (compare with Eq. (4.4)) of the single particle expectation value $x_{123}^{(3)}$, equation (4.7b). With increasing T and P, the cubic crystal field becomes more spherical which leads to a decrease of $x_{123}^{(3)}$. Despite these plausibility arguments we admit that the present theory does not prove the existence of a critical point. On the other hand it has been observed that the prolongation of the phase transition line beyond the critical point crosses the liquid-solid transition curve at its minimum. We expect that near the experimental critical point and beyond, the solid becomes more liquid like (dislocations). We feel that more detailed experimental information is needed which could serve as a guideline for the theory.

5 Lattice contraction

We now consider the Ce atoms located on a non rigid fcc lattice. We denote the lattice displacement of the Ce nucleus at site $\mathbf{n}$ by $\mathbf{u}(\mathbf{n})$. We assume that the core and valence electrons (in particular the $4f$ electron shell) follow adiabatically the nuclear displacements. Denoting the equilibrium nuclear positions by $\mathbf{X}(\mathbf{n})$, $\mathbf{n} = 1 - N$, we write for the $4f$ electron coordinates

$$\mathbf{R}(\mathbf{n}) = \mathbf{X}(\mathbf{n}) + \mathbf{r}(\mathbf{n}) + \mathbf{u}(\mathbf{n}). \tag{5.1}$$

We assume again that the electron is located on a sphere with radius $|\mathbf{r}(\mathbf{n})|$, centered around the nuclear position which now is $\mathbf{X}(\mathbf{n}) + \mathbf{u}(\mathbf{n})$. We start from the intersite Coulomb potential between $4f$ electrons and insert expression (5.1) into (2.8b). Expanding then in terms of nuclear displacements yields up to first order in $\mathbf{u}(\mathbf{n})$:

$$V(\mathbf{n},\mathbf{n}') = V(\mathbf{n},\mathbf{n}')\,|_{u=0} + \sum_{\nu} V_{\nu}(\mathbf{n},\mathbf{n}')[u_{\nu}(\mathbf{n}) - u_{\nu}(\mathbf{n}')], \tag{5.2}$$

where

$$V_\nu(\mathbf{n},\mathbf{n}') = \left.\frac{\partial V(\mathbf{n},\mathbf{n}')}{\partial X_\nu(\mathbf{n})}\right|_{u=0}, \tag{5.3}$$

$\nu = x, y, z$ being Cartesian indices. The term $V(\mathbf{n},\mathbf{n}')\mid_{u=0}$ corresponds to the interaction potential (2.8b), which has been studied in the previous sections. The coefficients $V_\nu(\mathbf{n},\mathbf{n}')$ still depend on the electronic configurations. Expansion in terms of SAF's $S_l^\tau(\hat{\mathbf{n}})$ leads to

$$V_\nu(\mathbf{n},\mathbf{n}') = \sum_{l\,l'}\sum_{\tau\,\tau'} v'^{\,\tau\tau'}_{\nu ll'}(\mathbf{n}-\mathbf{n}') S_l^\tau(\hat{\mathbf{n}}) S_{l'}^{\tau'}(\hat{\mathbf{n}}'), \tag{5.4}$$

where

$$v'^{\,\tau\tau'}_{\nu ll'}(\mathbf{n}-\mathbf{n}') = \int \mathrm{d}\Omega(\mathbf{n})\mathrm{d}\Omega(\mathbf{n}') V_\nu(\mathbf{n},\mathbf{n}') S_l^\tau(\hat{\mathbf{n}}) S_{l'}^{\tau'}(\hat{\mathbf{n}}'). \tag{5.5}$$

The contribution of the non rigid lattice to the intersite Coulomb potential now reads

$$U^{\mathrm{RRT}} = \frac{1}{2}\sum_{\mathbf{nn}'}\sum_{\nu}\sum_{l\,l'}\sum_{\tau\,\tau'} v'^{\,\tau\tau'}_{\nu ll'}(\mathbf{n}-\mathbf{n}') \times S_l^\tau(\hat{\mathbf{n}}) S_{l'}^{\tau'}(\hat{\mathbf{n}}')\,[u_\nu(\mathbf{n}) - u_\nu(\mathbf{n}')]. \tag{5.6}$$

In analogy with the corresponding interaction in molecular crystals [2], this contribution is referred to as rotation-rotation-translation (RRT) coupling. The lattice contraction that accompanies the orientational phase transition Fm$\bar{3}$m → Pa$\bar{3}$ in solid C_{60} has been studied before by experiment [55] and by theory [53], and the following considerations are inspired by analogies with orientational phase transitions.

In the following we restrict ourselves to quadrupolar interactions $l = 2$ of T_{2g} symmetry. Proceeding as in Section 2 we rewrite expression (5.6) as an operator in the space of $4f$ electrons, $U^{\mathrm{QQT}} \doteq U^{\mathrm{RRT}}$:

$$U^{\mathrm{QQT}} = \frac{1}{2}\sum_{\mathbf{nn}'} \rho^{(k)}(\mathbf{n}) v'^{\,kk'}_{\nu 22}(\mathbf{n}-\mathbf{n}') \rho^{(k')}(\mathbf{n}')[u_\nu(\mathbf{n}) - u_\nu(\mathbf{n}')]. \tag{5.7}$$

Here summation is understood over repeated indices ν, k, k'. The indices $k(k')$ refer to the three T_{2g} components. The electronic density operator is defined by

$$\rho^{(k)}(\mathbf{n}) = \sum_{ij} c_2^{(k)}(ij)\rho_{ij}(\mathbf{n}), \tag{5.8}$$

where $i(j)$ are the electronic states. We rewrite the interaction (5.7) in reciprocal space. The Fourier expansion of the nuclear displacements reads

$$\mathbf{u}(\mathbf{n}) = (Nm)^{-1/2}\sum_{\mathbf{q}} \mathbf{u}(\mathbf{q})\mathrm{e}^{i\mathbf{q}\cdot\mathbf{X}(\mathbf{n})}, \tag{5.9}$$

where m is the nuclear mass and N the total number of Ce atoms in the lattice. Defining

$$\rho^{(k)}(\mathbf{q}) = \sum_{ij} c_2^{(k)}(ij)\rho_{ij}(\mathbf{q}), \tag{5.10}$$

(compare with Eqs. (3.8a–c)), we obtain

$$U^{\mathrm{QQT}} = \frac{i}{2}\sum_{\mathbf{q}}\sum_{\mathbf{p}} v'^{\,kk'}_{\nu 22}(\mathbf{q},\mathbf{p})\rho^{(k)}(-\mathbf{p}-\mathbf{q})\rho^{(k')}(\mathbf{p})u_\nu(\mathbf{q}), \tag{5.11}$$

where

$$v'^{\,kk'}_{\nu 22}(\mathbf{q},\mathbf{p}) = (Nm)^{-1/2}\sum_{\boldsymbol{\kappa}} v'^{\,kk'}_{\nu 22}(\boldsymbol{\kappa}) \times \cos\left[\left(\mathbf{p}+\frac{\mathbf{q}}{\mathbf{2}}\right)\cdot\mathbf{X}(\boldsymbol{\kappa})\right]\sin\left[\frac{\mathbf{q}\mathbf{X}(\boldsymbol{\kappa})}{2}\right]. \tag{5.12}$$

Here $\boldsymbol{\kappa}$ stands for $(\mathbf{n}-\mathbf{n}')$ and $\mathbf{X}(\boldsymbol{\kappa})$ for $\mathbf{X}(\mathbf{n}) - \mathbf{X}(\mathbf{n}') = \mathbf{X}(\mathbf{n}-\mathbf{n}')$. Exploiting the periodicity of the rigid lattice, we see that the summation over κ corresponds to the summation over the neighbors $\mathbf{n}'$ of the site $\mathbf{n}$. In the following we restrict ourselves to twelve nearest neighbors on the fcc lattice. In Section 3 we have seen that the orientational phase transition is driven by the condensation scheme (3.9a, b) at the X point of the Brillouin zone. In the long wavelength limit $\mathbf{q} \to 0$, and for $\mathbf{p}$ close to the star of $\mathbf{p}^{\mathrm{X}}$, expression (5.11) becomes diagonal in k:

$$U^{\mathrm{QQT}} = i\sum_{\mathbf{qp}}\sum_{\nu(k)}{}' v'^{\,kk}_{\nu 22}(\mathbf{q},\mathbf{p})\rho^{(k)}(-\mathbf{p})\rho^{(k)}(\mathbf{p})u_\nu(\mathbf{q}). \tag{5.13}$$

Here the sum $\sum'$ refers to $\nu = x, y$ for $k = 3$, to $\nu = z, x$ for $k = 2$ and to $\nu = x, y$ for $k = 1$ (compare with the condensation scheme). The coupling matrix reduces to

$$v'^{33}_{\nu}(\mathbf{q},\mathbf{p}) = (Nm)^{-1/2}\Lambda q_\nu a\cos\left(\frac{p_x a}{2}\right)\cos\left(\frac{p_y a}{2}\right) \tag{5.14}$$

for $\nu = x$ or y. The expressions for v'^{22}_{ν} and v'^{11}_{ν} follow by permutation of indices. The coupling constant Λ is given by equation (5.5) for the particular case

$$\Lambda = v'^{33}_{\nu}(\boldsymbol{\kappa}), \tag{5.15}$$

where $\nu = x$ or y and $\mathbf{X}(\boldsymbol{\kappa}) = (a/2)(1,1,0)$. Notice that $v'^{22}_{\nu}(\boldsymbol{\kappa})$ and $v'^{11}_{\nu}(\boldsymbol{\kappa})$ have the same value Λ for $\nu = z$ or x and $\mathbf{X}(\boldsymbol{\kappa}) = (a/2)(1,0,1)$ and for $\nu = z$ or y and $\mathbf{X}(\boldsymbol{\kappa}) = (a/2)(0,1,1)$, respectively. These properties reflect the symmetry of the T_{2g} functions and of the fcc lattice. We find, by using the Coulomb potential (2.8b):

$$\Lambda = -445\ \mathrm{K}/\text{Å}. \tag{5.16}$$

Proceeding as in reference [53], we find that the QQT interaction leads to an additional contribution to the free energy per atom:

$$F^{\mathrm{QQT}}[\varepsilon,\rho] = -2a\Lambda\rho^2(\varepsilon_{xx} + \varepsilon_{yy} + \varepsilon_{zz}) \tag{5.17}$$

where $\varepsilon_{\nu\nu}$ are the longitudinal strains and ρ the quadrupolar order parameter amplitude. Combining $F^{\mathrm{QQT}}[\varepsilon,\rho]$

with the elastic contribution $F^{\mathrm{TT}}[\varepsilon]$ to the free energy of a cubic lattice, we obtain that minimization of the free energy leads to

$$\varepsilon_{xx} = \varepsilon_{yy} = \varepsilon_{zz} = 8a^{-2}\Lambda\kappa_L\rho^2, \tag{5.18}$$

where $\kappa_L = (c_{11}^0 + 2c_{12}^0)^{-1}$ is the bare linear compressibility and c_{11}^0 and c_{12}^0 are the elastic constants. Since $\Lambda < 0$, we find that equation (5.18) accounts for a contraction of the lattice in the cubic direction at the first order transition $\gamma \to \alpha$. From equation (5.18) we obtain that the change of the lattice constant a at the transition is given by $\Delta a = a\varepsilon_{xx} = -8|\Lambda|\kappa_L\rho^2/a$. With a bulk modulus [56] $(3\kappa_L)^{-1} = 101.6$ kbar we find a contraction $\Delta a \approx -0.001$ Å. Although the present theory gives the correct sign, the numerical value is about two orders of magnitude smaller than experimental values. However, we should keep in mind that within the present approach the lattice deformation is treated as a perturbation of the rigid lattice only. Experimentally there is evidence for a partial or incomplete softening of the $\gamma-$Ce lattice as the $\gamma \to \alpha$ transition is approached with decreasing temperature (for a review see Sect. 2.4.5 in Ref. [4]). Beside the coupling U^{QQT} we are considering here, there exists also a bilinear coupling U^{QT} between quadrupolar fluctuations of $\mathrm{T_{2g}}$ or $\mathrm{E_g}$ symmetry and the corresponding shear strains. Such bilinear coupling, which are well known in Jahn-Teller systems [57] and in molecular crystals [58] can act as driving mechanism of a structural phase transition where the lattice structure changes from cubic to lower symmetry (say, orthorhombic etc.). Since the lattice structure in the $\gamma \to \alpha$ transition of Ce remains fcc, the coupling U^{QT} cannot be the driving mechanism, however its presence should lead to partial softening phenomena [56]. A self consistent approach which takes systematically into account the interplay between quadrupolar ordering and a partial softening of the lattice would lead to an increase of lattice contraction. Such a self-consistent calculation is beyond the scope of the present work.

In reference [53] the Clausius-Clapeyron equation has been derived and it has been shown that the transition temperature T_1 is a linear function of external pressure P with a positive coefficient of the proportionality. The theory then can be applied to the phase transition in cerium with

$$\frac{\mathrm{d}T_1}{\mathrm{d}P_1} = 4a|\Lambda|\kappa_L x^{(2)}, \tag{5.19}$$

which accounts for the linear pressure increase of the γ/α boundary of the PT diagram of cerium [4].

6 Conclusions

We have calculated the crystal field of $\gamma-$Ce which is in good correspondence with experiment. We have studied anisotropic quadrupolar interactions associated with quantum transitions of localized $4f$ electrons in cerium. We have found that the $\gamma-\alpha$ phase transition can be described in terms of condensation of quadrupolar density fluctuations according to the $\mathrm{Fm\bar{3}m} \to \mathrm{Pa\bar{3}}$ scheme. The phase transition is of first order. The coupling of electronic quadrupolar density fluctuations to lattice displacements leads to a contraction of the cubic lattice at the transition. We find that the transition temperature increases linearly with pressure. Quadrupolar ordering combined with a coupling to lattice displacements could possibly account for transitions to phases of lower symmetry than $\mathrm{Pa\bar{3}}$. On the basis of our study of $4f$ charge density fluctuations in the disordered γ phase the following classification of other phases of cerium seems plausible. The tetragonal phase [25,4] which is reached under some conditions with applied pressure can be attributed to the condensation of the X_2^+ mode discussed in Section 3 and Appendix C. The condensation scheme $\mathrm{Fm\bar{3}m} \to \mathrm{Pmnn}$ where only two components condense at a single arm of the X point [51], for example $\rho^{(1)\mathrm{e}}(\mathbf{q}_z^{\mathrm{X}})$ and $\rho^{(2)\mathrm{e}}(\mathbf{q}_z^{\mathrm{X}})$, (3.8c) could lead to the orthorhombic α' phase [26,4] of cerium.

Quadrupolar interactions between density fluctuations of $4f$, $3d$ and $2p$ degenerate orbitals can be used in a description of molecules and solids which goes beyond the standard Hartree-Fock scheme. The formalism which has been developed in the present paper can be applied to different quantum objects.

Our considerations have been based on the antiferrorotational ordering of electric quadrupoles which are due to quantum density fluctuations of the $4f$ electrons. The existence of the $\mathrm{Pa\bar{3}}$ symmetry of the ordered phase which we have assigned with α-Ce in the present theory can be checked by X-ray synchrotron radiation experiments. We are presently investigating the effect of quadrupolar interactions on magnetic properties.

We thank A.P.Murani and D.Schoemaker for helpful discussions about spin-orbit coupling. This work has been financially supported by the Fonds voor Wetenschappelijk Onderzoek, Vlaanderen, and the Onderzoeksfonds, Universiteit Antwerpen.

Note added in proof

Stassis *et al.* [59] have used polarized neutron scattering techniques to assess the spatial distribution and temperature dependence of the magnetization induced in a single crystal of cerium. They have found that the (200) reflection drops significantly at ≈ 100 K as a result of the $\gamma \to \alpha$ transformation, though other reflections are observed down to 90 K and no change in their scattering angles is detectable. These authors interpret their results as an indication that some ions of the $\gamma-$Ce crystal change their electronic configuration. Using the same technique Moon and Koehler [60] have studied the induced magnetization in the polycrystalline alloy $\mathrm{Ce_{0.736}Th_{0.264}}$ in both the γ and α phases. They have observed some impurity lines, the strongest of which could be indexed as a NaCl-type structure. Are these experiments an indication that the space group of α-Ce is different from $\mathrm{Fm\bar{3}m}$?

Appendix A

The spin-orbit coupling reads

$$V_{\rm so} = \zeta \mathbf{L}\mathbf{S} = \frac{\zeta}{2}\,\mathbf{L}\boldsymbol{\sigma} = \frac{\zeta}{2}\left\{L_z\sigma_z + \frac{1}{2}(L_+\sigma_+ + L_-\sigma_-)\right\}. \tag{A.1}$$

Here ζ is a spin-orbit coupling constant, $\boldsymbol{\sigma} = \{\sigma_1, \sigma_2, \sigma_3\}$ are Pauli spin matrices and $L_\pm = L_x \pm iL_y$, $\sigma_\pm = \sigma_x \pm i\sigma_y$. In the following we use $\zeta = 862$ K, which corresponds the experimentally detected splitting [7] $\Delta_{\rm so} \approx 260$ meV between the 6-fold degenerate level $J = 5/2$ and 8-fold degenerate $J = 7/2$. In the basis of spin-orbitals $\langle \hat{\mathbf{n}}|l = 3, m;\ \pm\frac{1}{2}\rangle$ the matrix elements of $V_{\rm so}$, (A.1) are given by

$$\begin{aligned}
\langle l, m';\ +\frac{1}{2}|V_{\rm so}|l, m;\ +\frac{1}{2}\rangle &= \ m\,\delta_{m,m'}\,(\zeta/2),\\
\langle l, m';\ -\frac{1}{2}|V_{\rm so}|l, m;\ -\frac{1}{2}\rangle &= -m\,\delta_{m,m'}\,(\zeta/2),\\
\langle l, m';\ -\frac{1}{2}|V_{\rm so}|l, m;\ +\frac{1}{2}\rangle &= \delta_{m,m'-1},\ (\zeta/2) \qquad\qquad (A.2)\\
&\qquad \times n\sqrt{(l+m)(l-m+1)},\\
\langle l, m';\ +\frac{1}{2}|V_{\rm so}|l, m;\ -\frac{1}{2}\rangle &= \delta_{m,m'+1}\,(\zeta/2)\\
&\qquad \times n\sqrt{(l-m)(l+m+1)},
\end{aligned}$$

where $n = -1$ for $m, m' > 0$ and $n = 1$ for $m, m' \leq 0$ since for Y_l^m we take the phase convention of reference [46]. Diagonalizing $V_{\rm so}$ one obtains two levels, $E_{\frac{5}{2}} = -1724$ K and $E_{\frac{7}{2}} = 1293$ K. The corresponding eigenvectors can be chosen in the form $\langle \hat{\mathbf{n}}|l = 3,\ s = \frac{1}{2};\ J, J_z\rangle$ given by the vector model for addition of orbital and spin momenta [47].

In a cubic crystal the free-ion energy levels are split by a crystal electric field. In our approach the crystal field $V_{\rm CF}$ is given by (2.4) and is a potential field experienced by a single $4f$ electron when only spherically symmetric Coulomb contributions ($l' = 0$) from neighboring sites and similar terms from the electronic density in the interstitial regions are taken into account. The crystal field has unit ($\rm A_{1g}$) cubic symmetry and does not possess explicit spin dependence. However, $V_{\rm CF}$ is not diagonal in the basis of $|l = 3,\ s = \frac{1}{2};\ \ J, J_z\rangle$. Therefore, the eigenfunctions and the energy spectrum of $V_0 = V_{\rm so} + V_{\rm CF}$, have to be obtained numerically by diagonalizing the corresponding matrix of V_0. $V_{\rm CF}$ can be written in the form similar to equation (2.21):

$$V_{\rm CF}(\mathbf{n}) = \Lambda \sum_{ij} \rho_{ij}(\mathbf{n}) c_l^{\rm A_{1g}}(ij) \tag{A.3}$$

where

$$\Lambda = \Lambda^{(\rm n)} + \Lambda^{(\rm core)} + \Lambda^{(\rm c)}_{\rm MT} + \Lambda^{(\rm c)}_i + \Lambda^{(f)}. \tag{A.4}$$

Here we distinguish two contributions from the conduction electrons, $\Lambda^{(\rm c)}_{\rm MT}$ being due to the band electron density inside a muffin-tin (MT) sphere with the radius $R_{\rm MT} = a/2\sqrt{2} = 3.448$ a.u. and $\Lambda^{(\rm c)}_i$ due to the uniformly distributed conduction electron density in the interstitial region. $\Lambda^{(\rm n)}$, $\Lambda^{(\rm core)}$, $\Lambda^{(f)}$ are due to nuclei, core and $4f$ contributions, respectively. For the latter term we have $\Lambda^{(f)} = \frac{12}{\sqrt{4\pi}} v^{\rm A_{1g}A_{1g}}_{l=4\,0}$, (we restrict ourselves to $l = 4$ in (2.21)), and similar expressions for $\Lambda^{(\rm n)}$, $\Lambda^{(\rm core)}$ and $\Lambda^{(\rm c)}_{\rm MT}$. Collecting these terms together we obtain

$$\Lambda^{(\rm n)} + \Lambda^{(\rm core)} + \Lambda^{(\rm c)}_{\rm MT} + \Lambda^{(f)} = \frac{12}{\sqrt{4\pi}} Q_{\rm MT}|v^{\rm A_{1g}A_{1g}}_{l=4\,0}|, \tag{A.5}$$

where $\rm Q_{MT} = +0.9136$ [45] is the total charge inside the MT sphere. From electrostatic considerations it follows that $\Lambda^{(\rm c)}_i$ is $\dfrac{\pi}{3\sqrt{2}-\pi} \approx 2.853$ times larger and of the same sign as the contribution from nearest MT spheres. As a result we have

$$\Lambda = \frac{46.236}{\sqrt{4\pi}} Q_{\rm MT}|v^{\rm A_{1g}A_{1g}}_{l=4\,0}| \approx 346\ \text{K}. \tag{A.6}$$

By means of relations (2.13), (2.5) we obtain

$$\begin{aligned}
V_{\rm CF}(\mathbf{n}) &= \Lambda \sum_{ij}\sum_{t\,t'} |i\rangle\langle i|t\rangle\langle t|S_4^{\rm A_{1g}}(\mathbf{n})|t'\rangle\langle t'|j\rangle\langle j|\\
&= \Lambda \sum_{ij}\sum_{t\,t'} \rho_{ij}(\mathbf{n}) c_4^{\rm A_{1g}}(t\,t')\langle i|t\rangle\langle t'|j\rangle,
\end{aligned} \tag{A.7}$$

where the symmetry adapted function $S_4^{\rm A_{1g}}$ reads [46]

$$S_4^{\rm A_{1g}}(\mathbf{n}) = \sqrt{\frac{7}{12}}\langle \hat{\mathbf{n}}|4, 0\rangle + \sqrt{\frac{5}{12}}\langle \hat{\mathbf{n}}|4, (4, c)\rangle, \tag{A.8}$$

the coefficients $c_4^{\rm A_{1g}}(t\,t') = \langle t|S_4^{\rm A_{1g}}(\mathbf{n})|t'\rangle$ are given in a basis of functions $\langle \hat{\mathbf{n}}|t\rangle$ and $\langle i|t\rangle$ defines the matrix of the corresponding unitary transformation. Of particular interest are the base functions where the spatial parts are given by the following symmetry adapted combinations [46] of $\langle \hat{\mathbf{n}}|l = 3, m\rangle$:

$$\begin{aligned}
\langle \hat{\mathbf{n}}|{\rm T_{1u}}, 1\rangle &= \sqrt{\frac{3}{8}}\langle \hat{\mathbf{n}}|3, (1, c)\rangle - \sqrt{\frac{5}{8}}\langle \hat{\mathbf{n}}|3, (3, c)\rangle,\\
\langle \hat{\mathbf{n}}|{\rm T_{1u}}, 2\rangle &= \sqrt{\frac{3}{8}}\langle \hat{\mathbf{n}}|3, (1, s)\rangle + \sqrt{\frac{5}{8}}\langle \hat{\mathbf{n}}|3, (3, s)\rangle,\\
\langle \hat{\mathbf{n}}|{\rm T_{1u}}, 3\rangle &= -\langle \hat{\mathbf{n}}|3, 0\rangle;
\end{aligned} \tag{A.9}$$

$$\begin{aligned}
\langle \hat{\mathbf{n}}|{\rm T_{2u}}, 1\rangle &= -\sqrt{\frac{5}{8}}\langle \hat{\mathbf{n}}|3, (1, c)\rangle - \sqrt{\frac{3}{8}}\langle \hat{\mathbf{n}}|3, (3, c)\rangle,\\
\langle \hat{\mathbf{n}}|{\rm T_{2u}}, 2\rangle &= \sqrt{\frac{5}{8}}\langle \hat{\mathbf{n}}|3, (1, s)\rangle - \sqrt{\frac{3}{8}}\langle \hat{\mathbf{n}}|3, (3, s)\rangle,\\
\langle \hat{\mathbf{n}}|{\rm T_{2u}}, 3\rangle &= \langle \hat{\mathbf{n}}|3, (2, c)\rangle;
\end{aligned} \tag{A.10}$$

$$\langle \hat{\mathbf{n}}|{\rm A_{2u}}\rangle = \langle \hat{\mathbf{n}}|3, (2, s)\rangle. \tag{A.11}$$

We recall that $\mathrm{T_{1u}}$, $\mathrm{T_{2u}}$ and $\mathrm{A_{2u}}$ are irreducible representations of the cubic group $\mathrm{O_h}$. We construct the basis which we will call crystal field representation in the following way. As first 7 functions $\langle \hat{\mathbf{n}}|t\rangle$ we take $\langle \hat{\mathbf{n}}|\mathrm{T_{1u}},1\rangle u(s_z)$, ... , $\langle \hat{\mathbf{n}}|\mathrm{A_{2u}},1\rangle u(s_z)$ in the order (A.9–A.11) with the spin component $s_z = +\frac{1}{2}$. As functions $\langle \hat{\mathbf{n}}|t\rangle$, $t = 8 - 14$ we take the same functions (A.9–A.11) with the other spin component $s_z = -\frac{1}{2}$. In the crystal field representation we have

$$c_4^{\mathrm{A_{1g}}}(t\,t') = c_4^{\mathrm{A_{1g}}}(t\,t)\,\delta_{t\,t'}, \tag{A.12}$$

where $c_4^{\mathrm{A_{1g}}}(t\,t) = c(\mathit{\Gamma}_t)$ depends only on the representation $\mathit{\Gamma}_t = \mathrm{A_{2u}}, \mathrm{T_{1u}}, \mathrm{T_{2u}}$. We have obtained $c(\mathrm{A_{2u}}) = -0.23505$, $c(\mathrm{T_{1u}}) = 0.11752$ and $c(\mathrm{T_{2u}}) = -0.03917$. Applying (A.12) to (A.7) we find

$$V_{\mathrm{CF}}(\mathbf{n}) = \sum_{ij}\sum_{t} \rho_{ij}(\mathbf{n})\langle i|t\rangle \varepsilon_t^{\mathrm{CF}}\langle t|j\rangle, \tag{A.13}$$

where

$$\varepsilon_t^{\mathrm{CF}} = \mathit{\Lambda}\, c(\mathit{\Gamma}_t). \tag{A.14}$$

The form (A.13) implies that the operator $V_{\mathrm{CF}}(\mathbf{n})$ is diagonal in the crystal field representation. In the absence of the spin-orbit coupling V_{so} the single particle energy spectrum is given by (A.14). We have obtained $\varepsilon^{\mathrm{CF}}(\mathrm{A_{2u}}) = -81.3$ K, $\varepsilon^{\mathrm{CF}}(\mathrm{T_{1u}}) = 40.7$ K and $\varepsilon^{\mathrm{CF}}(\mathrm{T_{2u}}) = -13.6$ K.

Carrying out numerical calculations we find convenient to use a basis where the spatial parts of the base functions $\langle \hat{\mathbf{n}}|b\rangle$, $b = 1 - 14$ are given by real spherical harmonics, (2.1a-2.1c). Namely, functions $b = 1 - 7$ are

$$\begin{aligned} &Y_3^0 u(s_z),\; Y_3^{1,c}u(s_z),\; Y_3^{2,c}u(s_z),\; Y_3^{3,c}u(s_z), \\ &Y_3^{1,s}u(s_z),\; Y_3^{2,s}u(s_z),\; Y_3^{3,s}u(s_z), \end{aligned} \tag{A.15}$$

with $s_z = +\frac{1}{2}$, while seven functions with the same spatial parts but $s_z = -\frac{1}{2}$ make $b = 8 - 14$. We consider matrices with elements $\langle b|V_{\mathrm{so}}|b'\rangle = V_{\mathrm{so}}(b\,b')$ and $\langle b|V_{\mathrm{CF}}|b'\rangle = V_{\mathrm{CF}}(b\,b')$:

$$\begin{aligned} V_{\mathrm{so}}(b\,b') &= \sum_{m\,m'}\sum_{s_z\,s_z'} \langle b|3,m,s_z\rangle \qquad \text{(A.16)} \\ &\quad \times \langle 3,m,s_z|V_{\mathrm{so}}|3,m',s_z'\rangle\langle 3,m',s_z'|b'\rangle, \\ V_{\mathrm{CF}}(b\,b') &= \sum_t \langle b|t\rangle\varepsilon_t^{\mathrm{CF}}\langle t|b'\rangle. \qquad \text{(A.17)} \end{aligned}$$

Here $\langle 3,m,s_z|V_{\mathrm{so}}|3,m',s_z'\rangle$ are given by (A.2) while unitary matrices $\langle b|3,m,s_z\rangle$, $\langle b|t\rangle$ of transformations can be deduced from equations (2.1a-2.1c) and (A.9-A.11). Incorporating $V_{\mathrm{so}}(b\,b')$ and $V_{\mathrm{CF}}(b\,b')$ in $V_0(b\,b')$, (2.3), we have solved the secular equation

$$\sum_{b'=1}^{14}\langle b|V_0|b'\rangle\langle b'|i\rangle = \varepsilon_i\,\langle b|i\rangle, \tag{A.18}$$

and have obtained the eigenvectors $\langle b|i\rangle$ and the eigenvalues ε_i, $i = 1 - 14$. The corresponding energy spectrum is given in Table 1.

Appendix B

Anisotropic quadrupolar contributions (that is, with $l = 2$, $l' = 2$) to the interaction $V(\mathbf{n},\mathbf{n}')$ arise due to localized $4f$ states. The fully occupied core shells have density

$$\rho_{\mathrm{core}}(\mathbf{r}) = \sum_{j_{occ}}\sum_{m_j} |\phi_j^{m_j}(r)|^2, \tag{B.1}$$

where j stands for total angular momentum quantum number. According to the generalized Unsöld theorem [48] each shell stays invariant under all rotations, *i.e.* closed shells have spherical symmetry. To be more precise, in a cubic environment $\rho_{\mathrm{core}}(\mathbf{r})$ has the symmetry $\mathrm{A_{1g}}$ of $\mathrm{O_h}$, and can be expressed in terms of symmetry adapted functions [46] with $l = 0, 4, \ldots$ However, deviations ($l = 4$, ...) due to cubic symmetry are negligible for the inner core electron density.

In the following we show that the application of the generalized Unsöld theorem [48] requires that the total electronic density of conduction electrons is an invariant of the cubic group $\mathrm{O_h}$. Leading terms are $l = 0, 4$, but the main contribution is also isotropic, $l = 0$. A metallic wave function $\psi_n(\mathbf{k}|\mathbf{r})$ is given by a band index n and a wave vector $\mathbf{k}$ of the Brillouin zone (BZ) and the corresponding eigenvalue (band energy) is $E_n(\mathbf{k})$. The total metallic electronic density reads

$$\rho_m(\mathbf{r}) = \sum_{E_n(\mathbf{k})\leq \mathrm{E_F}} \psi_n^*(\mathbf{k}|\mathbf{r})\,\psi_n(\mathbf{k}|\mathbf{r}), \tag{B.2}$$

where the summation is taken over all states in the Brillouin zone for all energies smaller than the Fermi energy $\mathrm{E_F}$. In the following we will perform the summation in (B.2) in two stages. First, we distinguish the contributions from electronic states with the same degenerate value $\lambda \equiv E_n(\mathbf{k})$. Apart from accidental degeneracies $E_{n'}(\mathbf{k}') = E_n(\mathbf{k})$ the corresponding wave functions are known to form the basis of an irreducible representation of the space group $\mathrm{G} \equiv \mathrm{Fm\bar{3}m}$. Indeed, for the chosen value of $\mathbf{k}_1 = \mathbf{k}$ there is a set $\psi_{\mathbf{k}_1,1}$, $\psi_{\mathbf{k}_1,2}$, ... $\psi_{\mathbf{k}_1,t}$ of t degenerate eigenfunctions with the eigenvalue λ, which form a small representation ($\mathit{\Gamma}_p^{\mathbf{k}_1}$) of the little group of $\mathbf{k}_1$. (We use notations and definitions of the Ref. [46]). In the physical approach one can say that there is a similar set of t degenerate eigenfunctions with the same eigenvalue λ at each of the other wave vectors $S\mathbf{k}_1$ in the star of $\mathbf{k}_1$, where S is a point-group operator. In the stricter mathematical approach there is a set of (qt) eigenfunctions with the eigenvalue λ,

$$\{T_j|\mathbf{x}_j\}\,\psi_{\mathbf{k}_1,i}(\mathbf{r}), \tag{B.3}$$

where $j = 1 - q$ describes different components due to the star of $\mathbf{k}_1$ and $i = 1 - t$ is due to a small representation $\mathit{\Gamma}_p^{\mathbf{k}_1}$. (Here $\{T_j|\mathbf{x}_j\}$ are any set of left coset representatives of the little group of $\mathbf{k}_1$ in the space group G, see for details Ref. [46].) The $d = qt$ functions (B.3) form a basis of the irreducible representation of the space group $\mathrm{Fm\bar{3}m}$. The summation of squares of these functions gives an electronic density which according to the generalized Unsöld theorem [48] is an invariant of $\mathrm{Fm\bar{3}m}$. The same consideration holds for any energy level $E_{n'}(\mathbf{k}')$ of other space symmetry which accidentally coincides with $E_n(\mathbf{k})$. On the second stage we perform the summation in (B.2) on distinct values of $E_n(\mathbf{k}) \leq \mathrm{E_F}$. However, since all terms corresponding to different $E_n(\mathbf{k})$ are invariant, the total sum (B.2) possesses the full (unit) symmetry of $\mathrm{Fm\bar{3}m}$. Since the point group $\mathrm{O_h}$ is a subgroup of $\mathrm{Fm\bar{3}m}$, the total band electronic density, (B.2) will be invariant with respect to $\mathrm{O_h}$ and therefore at each lattice site $\mathbf{n}$ it can be expressed in terms of symmetry adapted functions of $\mathrm{A_{1g}}$ symmetry [46] with $l = 0, 4, \ldots$ These considerations can be generalized for double valued representations of the space group $\mathrm{Fm\bar{3}m}$ if a spin-orbit coupling and spin components of band electrons are taken into account.

We conclude that the quadrupolar electronic density with symmetry $\mathrm{T_{2g}}$ or $\mathrm{E_g}$ arises from transitions between the $4f$ localized states. There is no contribution to $l = 2$ terms from itinerant electrons with energies $E \leq \mathrm{E_F}$ which comprise the ground state of metal. The charge density of $\mathrm{A_{1g}}$ symmetry where the isotropic contribution with $l = 0$ is dominant, cannot couple to the quadrupolar density fluctuations at the X point of the Brillouin zone.

Appendix C

In the basis of functions $\langle \hat{\mathbf{n}}|b\rangle$, (A.15), the introduced coefficients $c_l^\tau(b\,b') = \langle b|S_l^\tau|b'\rangle$, (2.13, 2.14) are real and are cited in Table 2. The conversion to the functions $\langle \hat{\mathbf{n}}|i\rangle$ (see Appendix A) is given by the matrix elements $\langle b|i\rangle$, (A.18). However, the quantities $y^{(2)}(\mathrm{X}_2^+)$, $y^{(2)}(\mathrm{X}_5^+) = x^{(2)}$, $x_{123}^{(3)}$, $x_{1111}^{(4)}$ and $x_{1122}^{(4)}$, (4.7a-4.7d) remain real. This holds because for real functions S_2^τ (2.15a-2.16c) we obtain $c_2^\tau(ij)^* = c_2^\tau(ji)$, equation (2.13). Besides, two matrices $\langle i|S_{l=2}^\tau(ij)|j\rangle$ are imaginary (for $\tau = \mathrm{T_{2g}}, 1$ and $\tau = \mathrm{T_{2g}}, 3$) and the other ($\tau = \mathrm{T_{2g}}, 2$) is real. We recall that $y^{(2)}(\mathrm{X}_5^+)/T$ and $y^{(2)}(\mathrm{X}_2^+)/T$ are single particle susceptibilities of X_5^+ and X_2^+ modes, respectively (Sect. 3). In the case of complete degeneracy where $\varepsilon_i = \varepsilon_0$ for all $i = 1-14$ the factor $\exp(-\varepsilon_0/T)$ can be taken out of the summations (4.7a)-(4.7d) and

$$\mathrm{e}^{-\varepsilon_0/T}/Z_0 = 1/14. \tag{C.1}$$

For this special case the quantities $y^{(2)}(\alpha)$ ($\alpha = \mathrm{X}_2^+, \mathrm{X}_5^+$), $x^{(2)}$, $x_{123}^{(3)}$, $x_{1111}^{(4)}$ and $x_{1122}^{(4)}$ are independent on the choice of basis. For example

$$\begin{aligned} y^{(2)}(\alpha) &= \frac{1}{14}\sum_{ij}\sum_{p_1,p_2}\sum_{p_3,p_4}\langle i|p_1\rangle c_2^{(k)}(p_1p_2)\langle p_2|j\rangle \\ &\quad\times\langle j|p_3\rangle c_2^{(k)}(p_3p_4)\langle p_4|i\rangle \qquad\qquad (\mathrm{C.2})\\ &= \frac{1}{14}\sum_{p_1,p_2}\sum_{p_3,p_4} c_2^{(k)}(p_1p_2)\, c_2^{(k)}(p_3p_4)\,\delta_{p_1p_4}\delta_{p_2p_3} \\ &= \frac{1}{14}\sum_{p_1p_2} c_2^{(k)}(p_1p_2)\, c_2^{(k)}(p_2p_1). \end{aligned}$$

Here $(k) = (\mathrm{E_g}, k = 1, 2)$ corresponds to the X_2^+ mode and $(k) = (\mathrm{T_g}, k = 1, 2, 3)$ to the X_5^+ mode. Using the Wigner-Eckart theorem [47,48] it is possible to show that for such case

$$y^{(2)}(\alpha) = x_0^{(2)} \equiv \frac{1}{15\pi} \approx 0.02122, \tag{C.3}$$

and is the same for density fluctuations of $\mathrm{E_g}$ and of $\mathrm{T_{2g}}$ type, (2.15a-2.16c). If the single particle energy spectrum of $V_0 = V_{\mathrm{so}} + V_{\mathrm{CF}}$ (see Appendix A) is taken into account then $y^{(2)}(\alpha)$ depends on temperature and deviates from the value $x_0^{(2)}$. In general then $y^{(2)}(\mathrm{X}_5^+) \neq y^{(2)}(\mathrm{X}_2^+)$. However, at the limit $T \to \infty$ the relation $y^{(2)}(\mathrm{X}_5^+) = y^{(2)}(\mathrm{X}_2^+) = x_0^{(2)}$ holds. With decreasing temperature we find that $y^{(2)}(\mathrm{X}_5^+)$ increases while $y^{(2)}(\mathrm{X}_2^+)$ decreases. At the temperature $T = 86$ K we obtain $x^{(2)} = y^{(2)}(\mathrm{X}_5^+) = 0.02334$ and $y^{(2)}(\mathrm{X}_2^+) = 0.01804$. Taking into account the corresponding eigenvalues, $\lambda_{\mathrm{X}_2^+}$ and $\lambda_{\mathrm{X}_5^+} = -\lambda^{\mathrm{X}}$ (Sect. 3) we conclude that the X_5^+ mode prevails and drives the phase transition $\mathrm{Fm\bar{3}m} \to \mathrm{Pa\bar{3}}$. Notice that in the other limiting case $T \to 0$, $y^{(2)}(\alpha) \neq 0$. Although at $T \to 0$ only the ground states $i = 1, 2$ of $\Gamma_7, 1$ (Tab. 1) become populated the intermediate summations in (4.7a-4.7d) include all allowed indices $j, h, l = 1-14$.

For the other quantities (4.7a-4.7d) of the leading X_5^+ mode we obtain $x_{123}^{(3)} = -1.303 \times 10^{-3}$, $x_{1111}^{(4)} = 8.266 \times 10^{-4}$, $x_{1122}^{(4)} = 4.921 \times 10^{-4}$. We find expansion coefficients $B = 8708$ K and $C = 71473$ K, (4.4, 4.5).

References

1. H.M. James, T.A. Keenan, J. Chem. Phys. **31**, 12 (1959); M. Yvinec, R.M. Pick, J. Phys. France **41**, 1045 (1980).
2. K.H. Michel, K. Parlinski, Phys. Rev. B **31**, 1823 (1985).
3. K.H. Michel, J.R.D. Copley, D.A. Neumann, Phys. Rev. Lett. **68**, 2929 (1992); K.H. Michel, Z. Phys. B Cond. Matter **88**, 71 (1992).
4. D.C. Koskenmaki, K.A. Gschneidner Jr., *Handbook on the Physics and Chemistry of Rare Earths*, edited by K.A. Gschneidner Jr., L. Eyring (Amsterdam, North-Holland, 1978), p. 337.
5. M.R. MacPherson, G.E. Everett, D. Wohlleben, M.B. Maple, Phys. Rev. Lett. **26**, 20 (1971).
6. D.C. Koskimaki, K.A. Gschneidner Jr., Phys. Rev. B **11**, 4463 (1975).
7. A.P. Murani, Z.A. Bowden, A.D. Taylor, R. Osborn, W.G. Marshall, Phys. Rev. B **48**, 13981 (1993).
8. W.H. Zachariasen, unpublished information (1949) quoted by A.W. Lawson, T.-Y. Tang, Phys. Rev. **76**, 301 (1949); L. Pauling, unpublished information (1950) quoted by A.F. Schuch, J.H. Sturdivant, J. Chem. Phys. **18**, 145 (1950).
9. D.R. Gustafson, J.D. McNutt, L.O. Roelling, Phys. Rev. B **183**, 435 (1969); R.F. Gempel, D.R. Gustafson, J.D. Willenberg, Phys. Rev. B **5**, 2082 (1972).
10. B. Johansson, Phil. Mag. **30**, 469 (1974).
11. U. Kornstädt, R. Lässer, B. Lengeler, Phys. Rev. B **21**, 1898 (1980).

12. J.W. Allen, S.J. Oh, I. Lindau, J.M. Lawrence, L.I. Johansson, S.B. Hagström, Phys. Rev. Lett. **46**, 1100 (1981); J.W. Allen, S.-J. Oh, I. Lindau, M.B. Maple, J.F. Suassuna, S.B. Hagström, Phys. Rev. B **26**, 445 (1982).
13. D.M. Wieliczka, C.G. Olson, D.W. Lynch, Phys. Rev. B **29**, 3028 (1984).
14. E. Weschke, C. Laubschat, T. Simmons, M. Domke, O. Strebel, G. Kaindl, Phys. Rev. B **44**, 8304 (1991).
15. J.K. Lang, Y. Bayer, P.A. Cox, Phys. Rev. Lett. **42**, 74 (1978); P.A. Cox, J.K. Lang, Y. Baer, J. Phys. F **11**, 113 (1981); J.K. Lang, Y. Baer, P.A. Cox, *ibid.* **11**, 121 (1981); Y. Baer, H.R. Ott, J.C. Fuggle, L.E. DeLong, Phys. Rev. B **24**, 5384 (1981).
16. E. Wuilloud, H.R. Moser, W.-D. Schneider, Y. Baer, Phys. Rev. B **28**, 7354 (1983).
17. J.C. Fuggle, F.U. Hillebrecht, J.-M. Esteva, R.C. Karnatak, O. Gunnarsson, K. Schönhammer, Phys. Rev. B **27**, 4637 (1983).
18. P.W. Anderson, Phys. Rev. **124**, 41 (1961).
19. O. Gunnarsson, K. Schönhammer, Phys. Rev. Lett. **50**, 604 (1983); O. Gunnarsson, K. Schönhammer, Phys. Rev. B **28**, 4315 (1983).
20. N.E. Bickers, D.L. Cox, J.W. Wilkins, Phys. Rev. B **36**, 2036 (1987).
21. D. Malterre, M. Grioni, Y. Baer, Adv. Phys. **45**, 299 (1996).
22. J.W. Allen, R.M. Martin, Phys. Rev. Lett. **49**, 1106 (1982).
23. J.W. Allen, L.Z. Liu, Phys. Rev. B **46**, 5047 (1992).
24. M. Lavagna, C. Lacroix, M. Cyrot, Phys. Lett. A **90**, 710 (1982); J. Phys. F **13**, 1007 (1985).
25. S. Endo, H. Sasaki, T. Mitsui, J. Phys. Soc. Jap. **42**, 882 (1977); N. Fujioka, S. Endo, N. Kawai, Phys. Lett. A **60**, 340 (1977).
26. W.H. Zachariasen, J. Appl. Phys. **48**, 1391 (1977); W.H. Zachariasen, F.H. Ellinger, Acta Cryst. A **33**, 155 (1977).
27. O. Gunnarsson, O. Jepsen, Phys. Rev. B **38**, 3568 (1988); O. Gunnarsson, K. Schönhammer, Phys. Rev. B **40**, 4160 (1989); L.Z. Liu, J.W. Allen, O. Gunnarsson, N.E. Christensen, O.K. Andersen, Phys. Rev. B **45**, 8934 (1992).
28. J.W. Allen, S.J. Oh, O. Gunnarsson, K. Schönhammer, M.B. Maple, M.S. Torikachvili, Adv. Phys. **35**, 275 (1986).
29. J.J. Joyce, A.J. Arko, J. Lawrence, P.C. Canfield, Z. Fisk, R.J. Bartlett, J.D. Thompson, Phys. Rev. Lett. **68**, 236 (1992).
30. J.M. Lawrence, A.J. Arko, J.J. Joyce, R.I.R. Blyth, R.J. Bartlett, P.C. Canfield, Z. Fisk, P.S. Riseborough, Phys. Rev. B **47**, 15460 (1993).
31. R.I.R. Blyth, J.J. Joyce, A.J. Arko, P.C. Canfield, A.B. Andrews, Z. Fisk, J.D. Thompson, R.J. Bartlett, P. Riseborough, J. Tang, J.M. Lawrence, Phys. Rev. B **48**, 9497 (1993); J.J. Joyce, A.B. Andrews, A.J. Arko, R.J. Bartlett, R.I.R. Blythe, C.G. Olson, P.J. Benning, P.C. Canfield, D.M. Poirier, Phys. Rev. B **54**, 17515 (1996).
32. A.B. Andrews, J.J. Joyce, A.J. Arko, J.D. Thompson, J. Tang, J.M. Lawrence, J.C. Hemminger, Phys. Rev. B **51**, 3277 (1995); A.B. Andrews, J.J. Joyce, A.J. Arko, Z. Fisk, *ibid.* **53**, 3317 (1996).
33. A.J. Arko, J.J. Joyce, A.B. Andrews, J.D. Thompson, J.L. Smith, D. Mandrus, M.F. Hundley, A.L. Cornelius, E. Moshopoulou, Z. Fisk, P.C. Canfield, A. Menovsky, Phys. Rev. B **56**, R7041 (1997).
34. O. Eriksson, R.C. Albers, A.M. Boring, G.W. Fernando, Y.G. Hao, B.R. Cooper, Phys. Rev. B **43**, 3137 (1991); Y. Baer, M. Grioni, D. Malterre, W.-D. Schneider, *ibid.* **44**, 9108 (1991); Weschke, C. Laubschat, R. Ecker, A. Höhr, M. Domke, G. Kaindl, L. Severin, B. Johansson, Phys. Rev. Lett. **69**, 1792 (1992); D. Malterre, M. Grioni, Y. Baer, L. Braicovich, L. Duo, P. Vavassori, G.L. Olcese, *ibid.* **73**, 2005 (1994); Weschke, C. Laubschat, R. Ecker, A. Höhr, M. Domke, G. Kaindl, L. Severin, B. Johansson, *ibid.* **73**, 2006 (1994).
35. O. Eriksson, M.S.S. Brooks, B. Johansson, Phys. Rev. B **41**, 7311 (1990); A.M. Boring, R.C. Albers, O. Eriksson, D.D. Koelling, Phys. Rev. Lett. **68**, 2652 (1992); Z. Szotek, W.M. Temmerman, H. Winter, *ibid.* **72**, 1244 (1994); A. Svane, *ibid.* **72**, 1248 (1994); T. Jarlborg, E.G. Moroni, G. Grimvall, Phys. Rev. B **55**, 1288 (1997); S.V. Beiden, W.M. Temmerman, Z. Szotek, G.A. Gehring, Phys. Rev. Lett. **79**, 3970 (1997).
36. R.I.R. Blyth, J.J. Joyce, A.J. Arko, Phys. Rev. Lett. **69**, 3418 (1992); D. Malterre, M. Grioni, P. Weibel, B. Dardel, Y. Baer, *ibid.* **69**, 3419 (1992); J.W. Allen, O. Gunnarsson, *ibid.* **70**, 1180 (1993); J.J. Joyce, A.J. Arko, *ibid.* **70**, 1181 (1993); L. Severin, B. Johansson, Phys. Rev. B **50**, 17886 (1994); N. Witkowski, F. Bertran, D. Malterre, *ibid.* **56**, 15040 (1997).
37. P. Morin, J. Magn. Magn. Mat. **71**, 151 (1988).
38. J.M. Effantin, J. Rossat-Mignod, P. Burlet, H. Bartholin, S. Kunii, T. Kasuya, J. Magn. Magn. Mater. **47&48**, 145 (1985).
39. M. Hiroi, S. Kobayashi, M. Sera, N. Kobayashi, S. Kunii, Phys. Rev. B **55**, 8339 (1997).
40. D. Gignoux, D. Schmitt, *Handbook on the Physics and Chemistry of Rare Earths*, edited by K.A. Jr. Gschneidner, L. Eyring (1995), Vol. 20, p. 355.
41. F.J. Ohkawa, J. Phys. Soc. Jap. **52**, 3897 (1983); **54**, 3909 (1985).
42. G. Uimin, Y. Kurampto, N. Fukushima, Solid State Commun. **97**, 595 (1996).
43. K.I. Kugel, D.I. Khomskii, Sov. Phys. JETP Lett. **15**, 446 (1972); Sov. Phys. JETP **37**, 725 (1973); M. Cyrot, C.Lyon-Caen, J. Phys. C (Solid State) **6**, L247 (1973); S. Inagaki, J. Phys. Soc. Jap. **39**, 596 (1975).
44. Calculations were performed within density functional theory (DFT) scheme with local density approximation (LDA) using a standard program for an atom of cerium in $6s^2 5d^1 4f^1$ configuration.
45. Calculations have been performed with the LAPW code used by G.V. Ionova, A.V. Nikolaev, Phys. Stat. Sol. B **162**, 451 (1990).
46. C.J. Bradley, A.P. Cracknell, *The Mathematical Theory of Symmetry in Solids* (Clarendon, Oxford, 1972).
47. E.P. Wigner, *Group Theory, and its application to the quantum mechanics of atomic spectra* (Academic Press, 1959).
48. M. Tinkham, *Group Theory and Quantum Mechanics* (McGraw-Hill, New York, 1964).
49. A.H. Millhouse, A. Furrer, Solid State Commun **15**, 1303 (1974).
50. K.H. Michel, J.R.D. Copley, Z. Phys. B Cond. Matter **103**, 369 (1997).
51. P. Zielinski, K. Parlinski, J. Phys. C **17**, 3287 (1984).
52. L.D. Landau, Phys. Z. Sowjetunion **11**, 26545 (1937); L.D. Landau, E.M. Lifshitz., *Statistical Physics*

(Pergamon, Bristol, 1995), Vol. 5.

53. D. Lamoen, K.H. Michel, Phys. Rev. B **48**, 807 (1993).
54. E.G. Ponyatovskii, Dokl. Akad. Nauk SSSR **120**, 1021 (1958).
55. W.I.F. David, R.M. Ibberson, T.J.S. Dennis, J.P. Hare, K. Prassides, Europhys. Lett. **18**, 219 (1992); P.A. Heiney, G.B.M. Vaughan, J.E. Fischer, N. Coustel, D.E. Cox, J.R.D. Copley, D.A. Neumann, W.A. Kamitakahara, K.M. Creegan, D.M. Cox, J.P. McCauley Jr., A.B. Smith III, Phys. Rev. B **45**, 4544 (1992).
56. F.F. Voronov, V.A. Goncharova, O.V. Stal'gorova, Sov. Phys. JETP **49**, 687 (1979).
57. M. Kataoka, J. Kanamori, J. Phys. Soc. Jap. **32**, 113 (1972); G.A. Gehring, K.A. Gehring, Rep. Prog. Phys. **38**, 1 (1975).
58. R.M. Lynden-Bell, K.H. Michel, Rev. Mod. Phys. **66**, 721 (1994).
59. C. Stassis, C.-K. Loong, G.R. Kline, O.D. McMasters, K.A. Gschneidner Jr., J. Appl. Phys. **49**, 2113 (1978).
60. R.M. Moon, W.C. Koehler, J. Appl. Phys. **50**, 2089 (1979).